LARGE SIGNAL TRANSIENT ANALYSIS OF DUTY RATIO CONTROLLED DC-TO-DC CONVERTER

by

Byungcho Choi

Thesis submitted to the Faculty of the

Virginia Polytechnic Institute and State University

in partial fulfillment of the requirements for the degree of

Master of Science

in

Electrical Engineering

APPROVED:

B. H. Cho, Chairman

F. C. Lee

V. Vorperian

March 10, 1988

Blacksburg, Virginia

LARGE SIGNAL TRANSIENT ANALYSIS OF DUTY RATIO CONTROLLED DC-TO-DC CONVERTER

by

Byungcho Choi

B. H. Cho, Chairman

Electrical Engineering

(ABSTRACT)

The large-signal transient response of duty ratio controlled dc-to-dc converters is investigated using the phase-plane technique.

The transition pattern of large-signal trajectories is provided in terms of the circuit parameters and operating conditions. Several transient trajectories of practical interest including start-up, step input voltage change and step-load change are analyzed. The effect of large-signal characteristics of the feedback controller on the transient trajectory is presented.

Acknowledgements

I would like to express the deepest gratitude to Dr. B.H. Cho for providing the opportunity to study the topic discussed in this thesis. His encouragement and suggestions were greatly appreciated.

I wish to express my appreciation to my committee members, Dr. F.C. Lee and Dr. V. Vorperian for their invaluable help.

With much love, I thank my parents and family for their understanding and patience for my academic pursuits.

Table of Contents

I. INTRODUCTION

To provide an efficient power conversion, a dc-to-dc converter is composed of only reactive elements and high speed switches. The basic function of the converter, delivering energy from source to load in an efficient and regulated manner, is achieved by the suitable configuration of reactive elements and on-off action of switches. The existance of switches allows the converter to have several circuit structure. Depending upon the state of switches, the converter may have entirely different circuit configurations. Due to this inherent nature of changing the structure during the operation, a converter is a nonlinear time-variant system and does not lend itself to the direct application of the linear system theory. One of the most successful approachs for modeling the converter has been the state-space averaging technique whose principle is to replace the state-space representations of two linear systems by a single state-space representation under the small-signal assumption. The small-signal model derived from the state-space averaging technique enables one to apply linear system control theories such as Bode plot, root locus and pole placement technique to design the feedback controller which provides the optimum small-signal characteristics. However, the small-signal model can not describe the behaviour of

the converter during a large transient. The small-signal approximation which is the crucial step of the state-space averaging technique is no longer valid in large transient.

Unfortunately, since there is no general model which can describe the large-signal characteristics of the converter, most of the design procedure is based on the small-signal model. It is, therefore, quite possible to design a converter which results in an unacceptable or unstable large transient response in spite of its excellent small-signal performance. Therefore, it is imperative to understand the large-signal behaviour of the converter to design one which has acceptable large-signal responses as well as the desired small-signal characteristics.

The large-signal characteristic of the converter has been investigated by several people. D.B. Edward investigated the global stability problem of the buck converter using the second method of Liapunov and derived the sufficient condition for global stability [1]. R.W. Erickson derived a set of nonlinear state equations which describe the converter in large transient by using the averaged equation without any small-signal assumption. He showed that a boost converter could be stable for small signal but unstable for large signal [2]. In Reference [3], K. Harada analyzed the start-up and step load change response of buck converter. W.W. Burns. III employed the phase-plane technique to study the qualitative behaviour of the converter [4,5,6]. Based on his analysis, he proposed a new conceptual converter control law which can, in theory, achieve steady state operation with one switching cycle regardless of the initial condition. More recently, Ram Venkataramanan employed the variable structure system theory to study the large-signal behaviour of converter [7]. He proposed the

sliding mode control law which can control the large-signal dynamic response of the converter using a switching line.

Despite numerous efforts to characterize large-signal behaviour of the converter, there is no general model or guideline which one can rely on during the converter design process. The main purpose of this thesis is to characterize the large-signal properties of the duty ratio controlled dc-to-dc converter. The phase-plane technique is employed with the aid of extensive computer simulation. The efforts are exerted to identify the pattern of transient trajectories of the converter in general (rather than analytical treatment of a specific topology or control method).

In Chapter II, the phase-plane technique is employed to study the qualitative characteristics of the converter. The phase-plane portraits of buck, boost and buck/boost are developed by considering the converter as a piecewise linear system which changes its structure by function of controller. The transition patterns of transient trajectories are investigated in Chapter III. The global behaviour of transient trajectories is explained. Making use of the concept developed in Chapter III, the important transient trajectories including start-up, step load change and step input voltage change trajectory are analyzed in Chapter IV. Finally, the effect of large-signal characteristics of the controller such as soft start circuit, duty ratio limitation and current limiting is presented in the Chapter V.

II . PHASE PLANE ANALYSIS OF DC-TO-DC CONVERTERS

2.1 Introduction

In this chapter, the phase-plane technique is employed to study the large-signal characteristics of the buck, boost and buck/boost converter. The phase-plane portraits are used to investigate the behaviours of a transient trajectories of the converters.

The dc-to-dc converter is viewed as a piecewise linear system changing its circuit configuration periodically. A particular circuit configuration of the converter at specific switching time instant is called the **subcircuit.** Depending upon the state of switches, the converter is broken down into several subcircuits. Each of these subcircuits is analyzed in the phase plane to yield the phase-plane portrait. By overplotting the phase-plane portraits of subcircuits, a complete phase-plane portrait of a

converter is presented. The large-signal behaviour of transient trajectory of a converter is discussed by the incorporation of the phase-plane portrait and the function of feedback controller.

In Section 2.2, the structure of buck, boost and buck/boost converters are investigated, leading to the introduction of four subcircuits which can identify those converters completely. The subcircuits are analyzed in the phase plane extensively in Section 2.3. In addition to the nature of the equilibrium point, the phase-plane portrait of each subcircuit is presented. The composite phase-plane portraits of converters are introduced in Section 2.4 by combining the phase-plane portraits of subcircuits. The start-up trajectories are explained providing considerable information about the transient behaviours of the converters. The phase-plane portraits and start-up trajectories of three basic converters (buck, boost and buck/boost) are compared.

2.2 Structure of DC-to-DC Converters

To provide an efficient power conversion, converters are composed of only non-dissipative devices such as inductors, capacitors and high speed switches. The suitable configuration of reactive elements and the appropriate method of controlling the switches enables the converter to work as a very efficient power conversion device. However, the existence of switches allows the converter to have several different circuit topologies during its operation. The basic converters such as buck, boost and buck/boost converters contain one transistor and one diode as switching devices. Depending upon the state of switches, a converter has several different circuit

configuration. These circuit configurations are classified into the following subcircuits.

- **On-time subcircuit** : Circuit configuration with transistor **on** and diode **off**
- **Off-time subcircuit** : Circuit configuration with transistor **off** and diode **on**
- **Zero inductor current subcircuit** : Circuit configuration with transistor **off** and diode **off**

Since the switches used in converters are all uni-directional, a third circuit configuration is possible in addition to on-time and off-time subcircuit. Whenever the inductor current is reduced to zero during the off-time subcircuit, the diode inhibits the reversal of the inductor current making both switches turn off. The circuit configuration under this situation is referred to as zero inductor current subcircuit.

The circuit diagrams of buck, boost and buck/boost converters are shown in Figs. 2.1, 2.2 and 2.3, respectively, and their various subcircuits are also included in the figures. A closer investigation of the structure of the basic three converters reveals that only four subcircuits are participating in forming the converters. In other words, all subcircuits of basic converters can be classified into four categories. Those four subcircuits are shown Fig. 2.4 where a different name is designated to each subcircuit for convenience. A specific combination of these subcircuits forms a particular converter such as buck, boost and buck/boost. For instance, subcircuits B, C and D constitute a complete buck converter. The combinations of subcircuits for basic converters are summarized in Table 2.1.

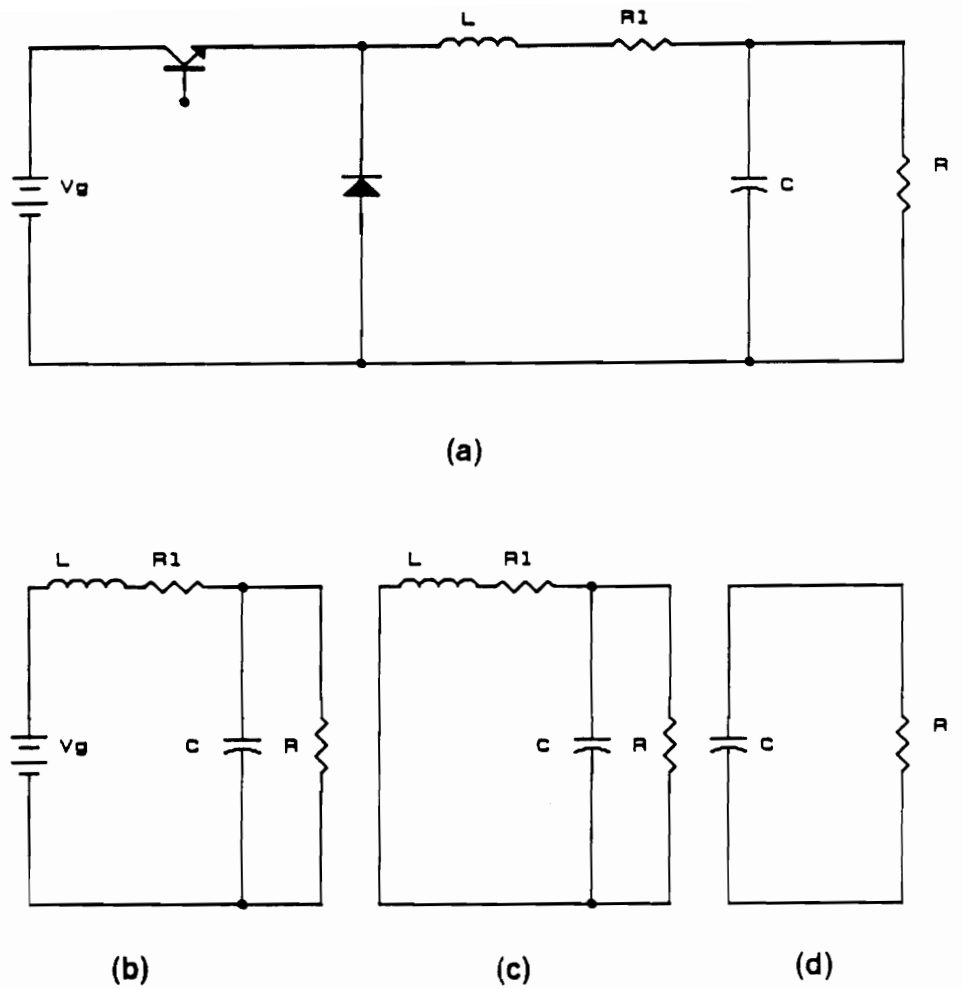

Figure 2.1 Buck converter and its subcircuits
(a) Buck converter (b) On-time subcircuit
(c) Off-time subcircuit (d) Zero inductor current subcircuit

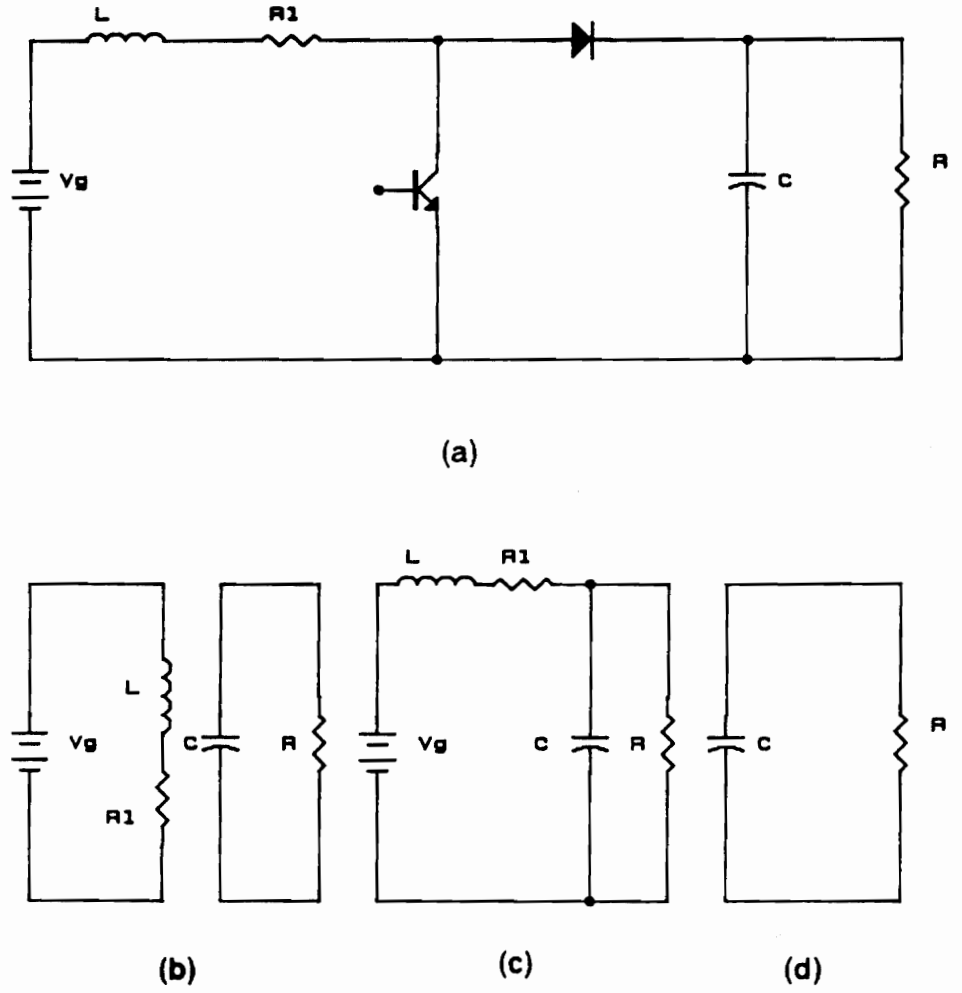

Figure 2.2 Boost converter and its subcircuits
(a) Boost converter (b) On-time subcircuit
(c) Off-time subcircuit (d) Zero inductor current subcircuit

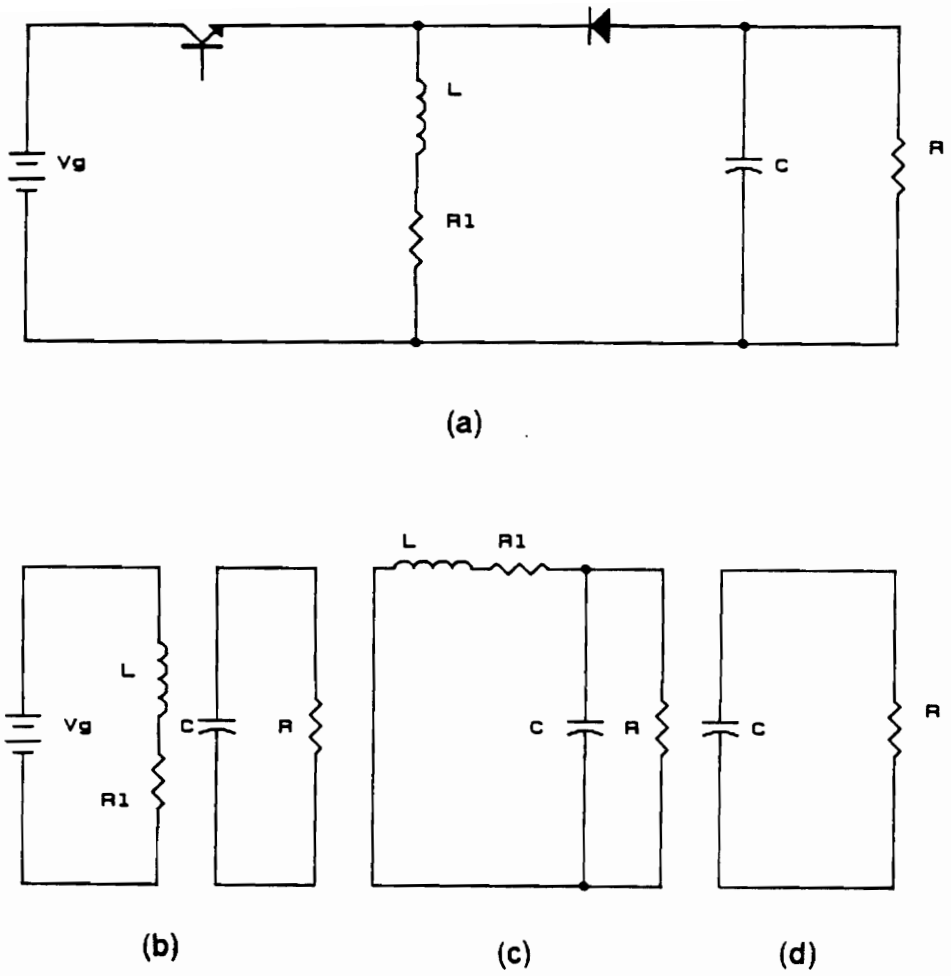

Figure 2.3 Buck/boost converter and its subcircuits
(a) Buck/boost converter (b) On-time subcircuit
(c) Off-time subcircuit (d) Zero inductor current subcircuit

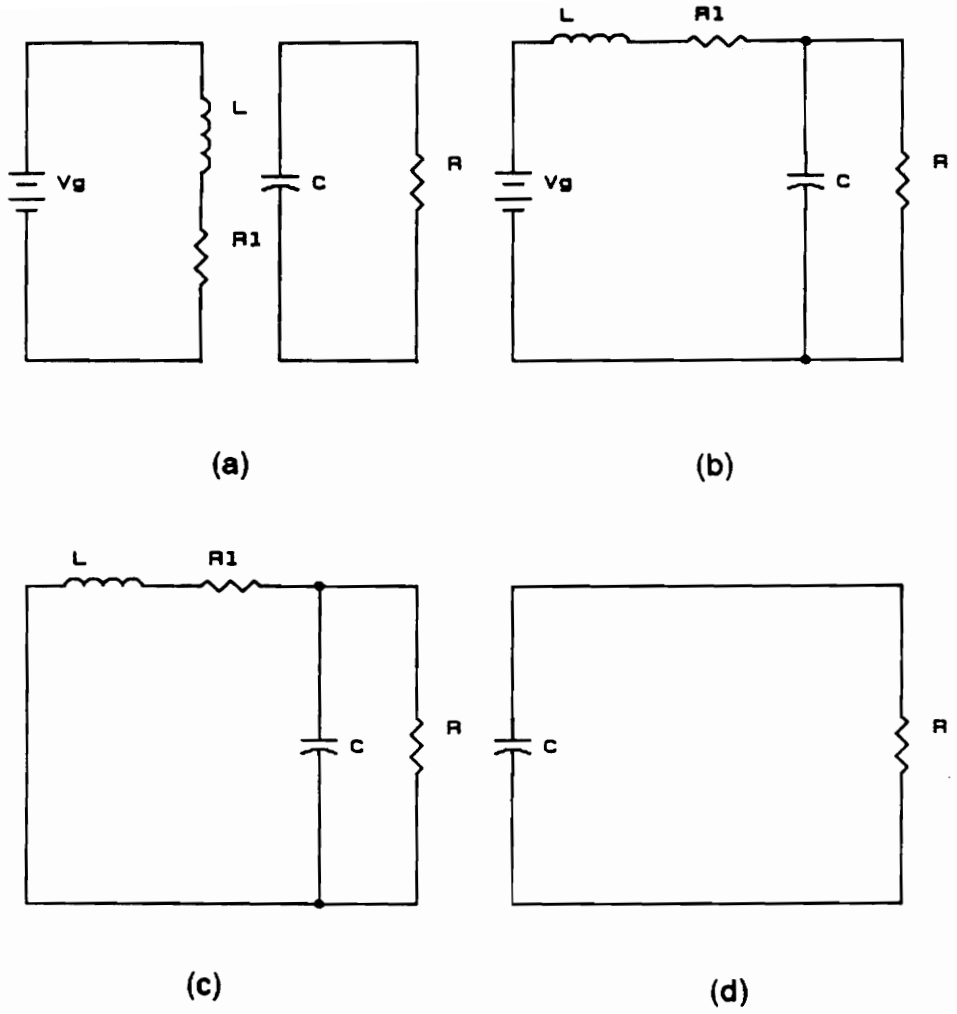

Figure 2.4 Four subcircuits of basic converters
(a) Subcircuit A (b) Subcircuit B
(c) Subcircuit C (d) Subcircuit D

TABLE 2.1

	On-time subcircuit	Off-time subcircuit	Zero inductor current subcircuit
Buck converter	Subcircuit B	Subcircuit C	Subcircuit D
Boost converter	Subcircuit A	Subcircuit B	Subcircuit D
Buck/Boost converter	Subcircuit A	Subcircuit C	Subcircuit D

2.3 Phase Plane Analysis of Subcircuits

The converter can have several circuit topologies during its operation. The circuit topology of the converter at particular instant of time was classified as on-time, off-time and zero inductor current subcircuit according to state of switches. The characteristics of subcircuits are different and the overall characteristics of the converter are quite different from those of subcircuits.

The converters are nonlinear and time-variant systems and do not lend themselves to the direct application of linear system theory because their special nature of changing structure during operation. The most efficient way to analyze this **periodically structure changing system** is to study all subcircuits separately and to combine their properties appropriately. After understanding the behaviour of each subcircuit, a clear idea of the behaviours of converters should be apparent by combining each subcircuit's characteristics. Even though a converter is a nonlinear system, its subcircuits are of a linear system whose characteristics can be precisely specified by a set of circuit parameters.

The phase-plane technique has several advantages in studying the time-variant system. The time information is suppressed or implicit in the phase-plane technique making the analysis much easier and more informative. Particularly, this technique is very handy for the second-order system and brings out the features of a system graphically.

A number of methods exist for the analytical construction of trajectories such as the vector field method or isoclines method. An alternative of these methods is to use

a computer to generate a family of trajectories with different initial conditions. The all phase-plane trajectories illustrated in this thesis were generated by a computer simulation using the EASY-5 software package developed by Boing Computer Service [8]. The structure of EASY-5 simulation is such that the particular circuit to be investigated is entered in terms of the system state equation. The state equation is integrated by means of the Euler Method to yield the time domain solution of system. The time-domain solutions are plotted in the phase plane to yield the trajectory of system.

2.3.1 Subcircuit A

The state equation of subcircuit A in Fig. 2.4 is

$$\begin{bmatrix} \dot{v}_C \\ \dot{i}_L \end{bmatrix} = \begin{bmatrix} \frac{-1}{RC} & 0 \\ 0 & \frac{-R_l}{L} \end{bmatrix} \begin{bmatrix} v_C \\ i_L \end{bmatrix} + \begin{bmatrix} 0 \\ \frac{1}{L} \end{bmatrix} V_g \qquad (2.1)$$

The capacitor voltage and inductor current are chosen as state of system in (2.1). By solving equation (2.1) for $\dot{v}_c = 0$ and $\dot{i}_L = 0$, we get the equilibrium point of system.

$$v_C = 0$$

$$i_L = \frac{V_g}{R_l}$$

Equation (2.1) can be transformed into a homogeneous version by changing variables.

$$\begin{bmatrix} \dot{\zeta}(t) \\ \dot{\eta}(t) \end{bmatrix} = \begin{bmatrix} \frac{-1}{RC} & 0 \\ 0 & \frac{-R_l}{L} \end{bmatrix} \begin{bmatrix} \zeta(t) \\ \eta(t) \end{bmatrix} \tag{2.2}$$

where

$$\zeta(t) = v_C(t)$$

$$\eta(t) = i_L(t) - \frac{V_g}{R_l}$$

Eigenvalues of (2.2) and corresponding eigenvectors are

$$\lambda_1 = \frac{-1}{RC} \quad , \quad U_1 = \begin{bmatrix} 1 \\ 0 \end{bmatrix}$$

$$\lambda_2 = \frac{-R_l}{L} \quad , \quad U_2 = \begin{bmatrix} 0 \\ 1 \end{bmatrix}$$

Note that, in usual power stage design, $\left| \frac{-R_l}{L} \right| < \left| \frac{-1}{RC} \right|$. The general solution of (2.2) is given by:

$$\chi = C_1 U_1 e^{\lambda_1 t} + C_2 U_2 e^{\lambda_2 t}$$

$$= e^{\lambda_2 t} (C_1 U_1 e^{(\lambda_1 - \lambda_2)t} + C_2 U_2) \tag{2.3}$$

$$(\lambda_1 < \lambda_2 < 0)$$

where

$$\underline{x} = \begin{bmatrix} \zeta(t) \\ \eta(t) \end{bmatrix}$$

$$\lambda_i \ , \ U_i \ : \ \textit{eigenpairs} \ (i = 1,2)$$

$$C_1 \ , \ C_2 \ : \ \textit{arbitrary constant}$$

From the equation (2.3), we can infer the behaviour of the solution of the system as follows.

- $\underline{x}$ approach to $\underline{0}$ as t approaches to the infinity.
- For a large t, $e^{(\lambda_1 - \lambda_2)t} << 1$

Therefore, $\underline{x}$ approaches to $\underline{0}$ a line through U_2 . In other words, $v_c(t)$ and $i_L(t)$ will approach to 0 and $\frac{V_g}{R_l}$, respectively, along the line through $v_c = 0$. A family of trajectories with given circuit parameter values are shown in Fig. 2.5. In this plot, $v_c(t)$ and $i_L(t)$, rather than $\zeta(t)$ and $\eta(t)$, are chosen as coordinates. The equilibrium point (0 , 150) is called the **stable node** . Note that, since every switch used in subcircuit A is uni-directional, only first quadrant is effective in the trajectory of DC-to-DC converter.

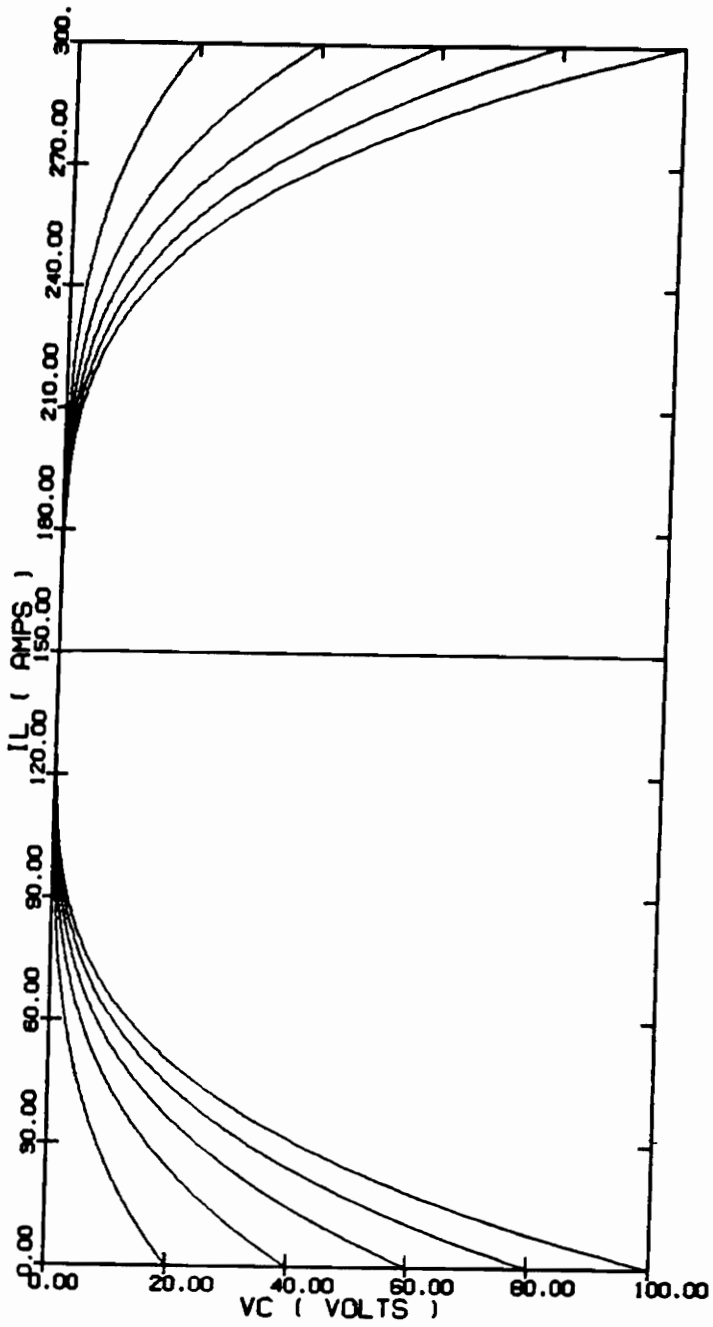

Figure 2.5 Phase plane portrait of subcircuit A
(L = 100 μH , C = 50 μF , Vg = 15 V , R = 5 Ω , R_l = 0.1 Ω)

2.3.2 Subcircuit B

The state equation of subcircuit B in Fig. 2.4 is

$$\begin{bmatrix} \dot{v}_C \\ \dot{i}_L \end{bmatrix} = \begin{bmatrix} \frac{-1}{RC} & \frac{1}{C} \\ \frac{-1}{L} & \frac{-R_l}{L} \end{bmatrix} \begin{bmatrix} v_C \\ i_L \end{bmatrix} + \begin{bmatrix} 0 \\ \frac{V_g}{L} \end{bmatrix} \tag{2.4}$$

The equilibrium point of (2.4) is

$$v_C = \frac{R}{R + R_l} V_g$$

$$i_L = \frac{V_g}{R + R_l}$$

With change of variables, we get the homogeneous version of (2.4)

$$\begin{bmatrix} \dot{\zeta}(t) \\ \dot{\eta}(t) \end{bmatrix} = \begin{bmatrix} \frac{-1}{RC} & \frac{1}{C} \\ \frac{-1}{L} & \frac{-R_l}{L} \end{bmatrix} \begin{bmatrix} \zeta(t) \\ \eta(t) \end{bmatrix} \tag{2.5}$$

where

$$\zeta(t) = v_C(t) - \frac{R}{R + R_l} V_g$$

$$\eta(t) = i_L - \frac{V_g}{R + R_l}$$

With practical converter circuit parameters, the eigenvalues of (2.9) turn out to be a complex conjugate pair.

$$\lambda_1 , \lambda_2 = \rho \pm i\mu$$

where

$$\rho = \frac{-(\frac{1}{RC} + \frac{R_l}{L})}{2} \qquad < 0$$

$$\mu = \frac{\sqrt{4(\frac{1}{LC} + \frac{R_l}{RCL}) - (\frac{1}{RC} + \frac{R_l}{L})^2}}{2} \qquad > 0$$

With the complex conjugate eigenvalues, the equilibrium point of (2.5) is a **stable spiral point.** The detailed discussion about the phase plane analysis of the subcircuit B is provided in the Appendix A. The general shape of phase plane portrait is shown in Fig. 2.6. Again, $v_c(t)$ and $i_L(t)$ are chosen as the coordinates of phase plane.

2.3.3 Subcircuit C and Subcircuit D

The subcircuit C has same structure as that of subcircuit B. The state equation of subcircuit C is

$$\begin{bmatrix} \dot{v}_C \\ \dot{i}_L \end{bmatrix} = \begin{bmatrix} \frac{-1}{RC} & \frac{1}{C} \\ \frac{-1}{L} & -\frac{R_L}{L} \end{bmatrix} \begin{bmatrix} v_C \\ i_L \end{bmatrix} \qquad (2.6)$$

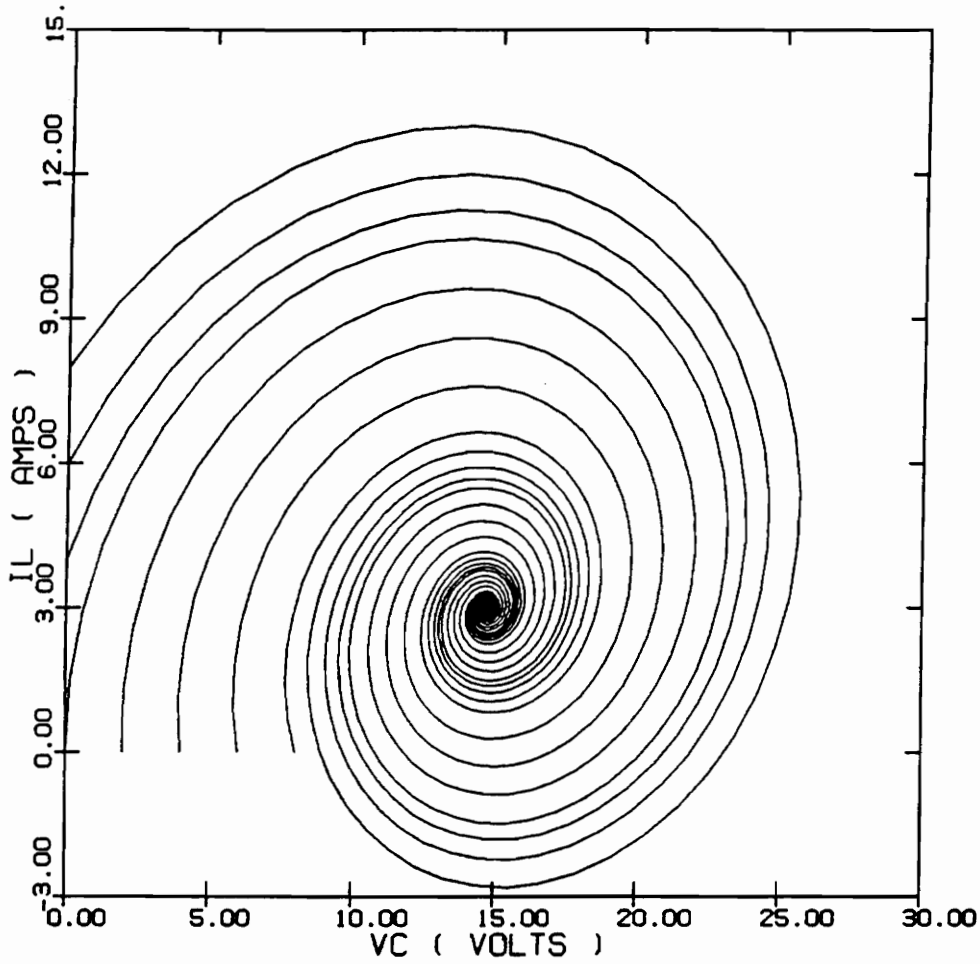

Figure 2.6 Phase plane portrait of subcircuit B
(L = 100 μH , C = 50 μF , Vg = 15 V , R = 5 Ω , R_l = 0.1 Ω)

A simple comparison of equation (2.6) and (2.4) shows that conclusion about the behaviour of subcircuit B can be directly applied to subcircuit C except that subcircuit C has its equilibrium point at the origin of phase plane. The computer generated phase plane portrait of subcircuit D with given parameter is given in Fig. 2.7.

The subcircuit D is effective whenever the inductor current reduces to zero during off-time subcircuit. In this subcircuit, the inductor current remains zero and the capacitor voltage decreases monotonously.

The state equation of subcircuit D is

$$\dot{v}_C = -\frac{v_C}{RC}$$

$$\dot{i}_L = 0 \tag{2.7}$$

And its solutions are

$$v_C(t) = V_C(0)\exp^{\frac{-t}{RC}}$$

$$i_L(t) = 0 \tag{2.8}$$

2.4 Phase Plane Portraits of DC-to-DC Converters

The time instant when the converter should change its circuit configuration from the one subcircuit to another subcircuit is determined by the feedback controller of converter. The controller, governed by a predetermined control law, generates a sequence of transistor on-off command during the converter's operation. As the

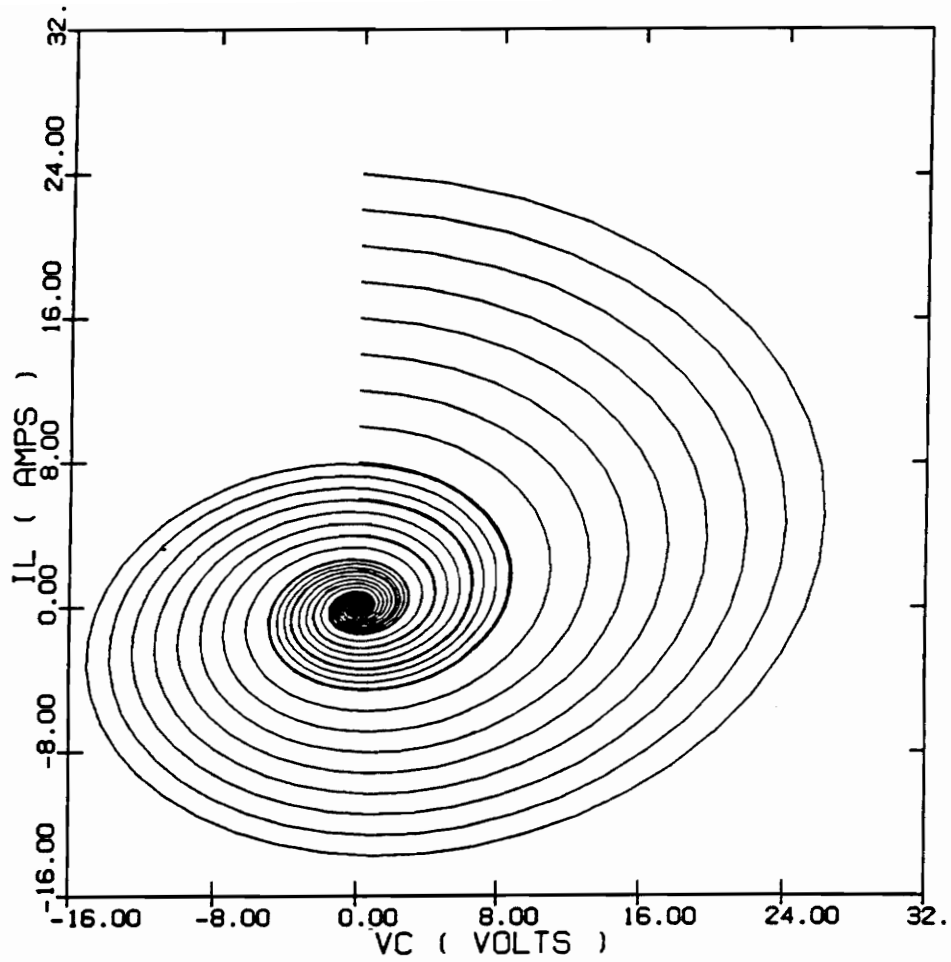

Figure 2.7 Phase plane portrait of subcircuit C
(L = 100 μH , C = 50 μF , Vg = 15 V , R = 5 Ω , R_l = 0.1 Ω)

converter changes the circuit configuration from one subcircuit to another subcircuit, its trajectory will follow the trajectories of the subcircuits accordingly. Consequently, any trajectory of a converter is composed of a sequence of trajectories of subcircuits and the phase-plane portraits of subcircuits constitute the phase-plane portrait of the converter. Based on the structure of three basic converters (buck, boost and buck/boost), four subcircuits were introduced with a comprehensive phase-plane analysis in the previous section. By overplotting the phase-plane portraits of the subcircuits, a composite phase-plane portrait of a converter will result.

The phase-plane portraits of four subcircuits with the following circuit parameters are in Fig. 2.8.

$L = 100\ \mu H$

$C = 50\ \mu F$

$R = 5\ \Omega$

$R_l = 0.1\ \Omega$

$V_g = 15\ V$

It is easy to see that the trajectory of subcircuit D is, simply, v_c axis in phase plane.

For the buck converter, the on-time subcircuit is subcircuit B and off-time subcircuit is subcircuit C. In figure 2.9, the phase-plane portrait of subcircuit B and C are over-plotted in the same plane resulting a complete phase-plane portrait of buck converter. A simplified **start-up** trajectory of the buck converter, (without considering any non-linearities of controller), is superimposed with bold line on this plot. Let's call the trajectory of on-time subcircuit of a converter **on-time trajectory**. Also, the trajectory

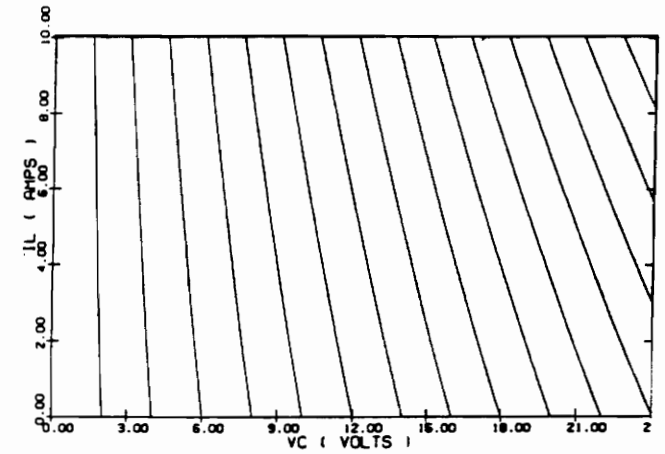

(a) Subcircuit A

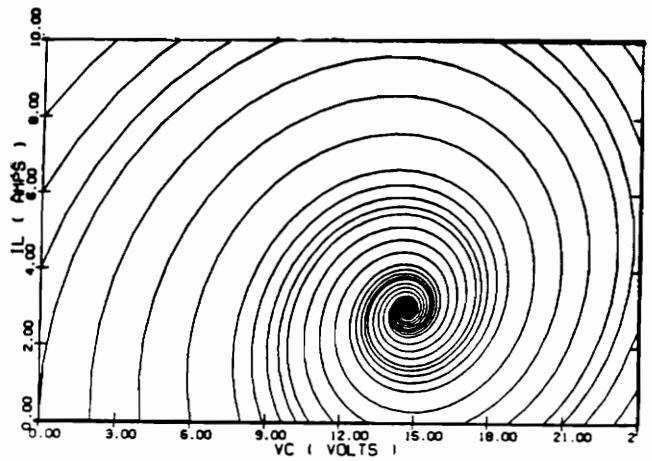

(b) Subcircuit B

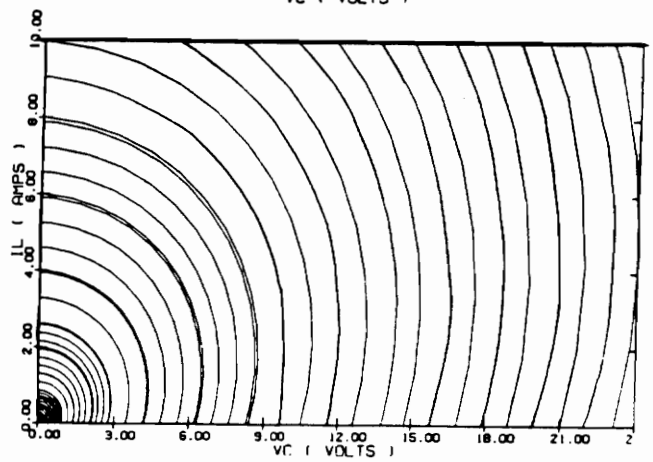

(c) Subcircuit C

Figure 2.8 Phase plane portrait of subcircuits
(a) Subcircuit A (b) Subcircuit B
(c) Subcircuit C

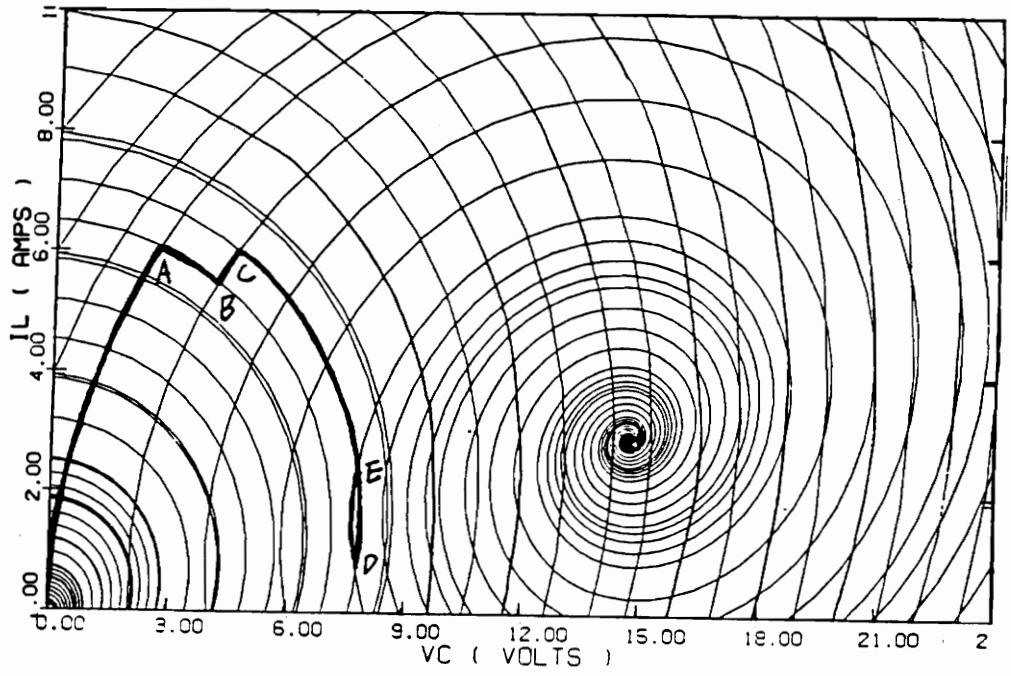

Figure 2.9 Phase plane portrait of buck converter and start-up trajectory

of off-time subcircuit and zero inductor current subcircuit will be called **off-time trajectory** and **zero inductor current trajectory**, respectively.

Starting from the origin, the state trajectory follows the on-time trajectory and off-time trajectory successively in attempting to reach the steady state trajectory by means of transistor on-off commands generated by the controller. Initially, the trajectory travels on-time trajectory. At point A, the controller generates the transistor-off command and trajectory starts to follow off-time trajectory up to the point B where the controller generates transistor on command again. From point B, the trajectory follows on-time trajectory again as illustrated. By repeating this process, the trajectory eventually arrives at the desired steady state trajectory. Once the converter starts its steady state operation, the trajectory will trace out a fixed segment of one of off-time trajectory and one of on-time trajectory periodically forming a closed path in the phase plane, namely, a steady state trajectory. The closed path of trajectory represents the desired steady state trajectory of buck converter.

Unlike the buck converter, the boost converter may have two different kinds of start-up trajectories. If the input voltage, V_g, is applied earlier than the transistor on-off command, the converter has been held the subcircuit B in Fig.2.4 with non-zero initial condition. Thus, the initial point of start-up trajectory is not the origin of the phase-plane but the equilibrium point of subcircuit B. In Fig. 2.10, the phase-plane portrait of subcircuit B and C are overplotted resulting a phase-plane portrait of a boost converter. A simplified start-up trajectory is depicted on the phase-plane portrait of converter assuming the situation explained above. The general behaviour of trajectory starting out at the equilibrium point of subcircuit B can be explained in the same way as before.

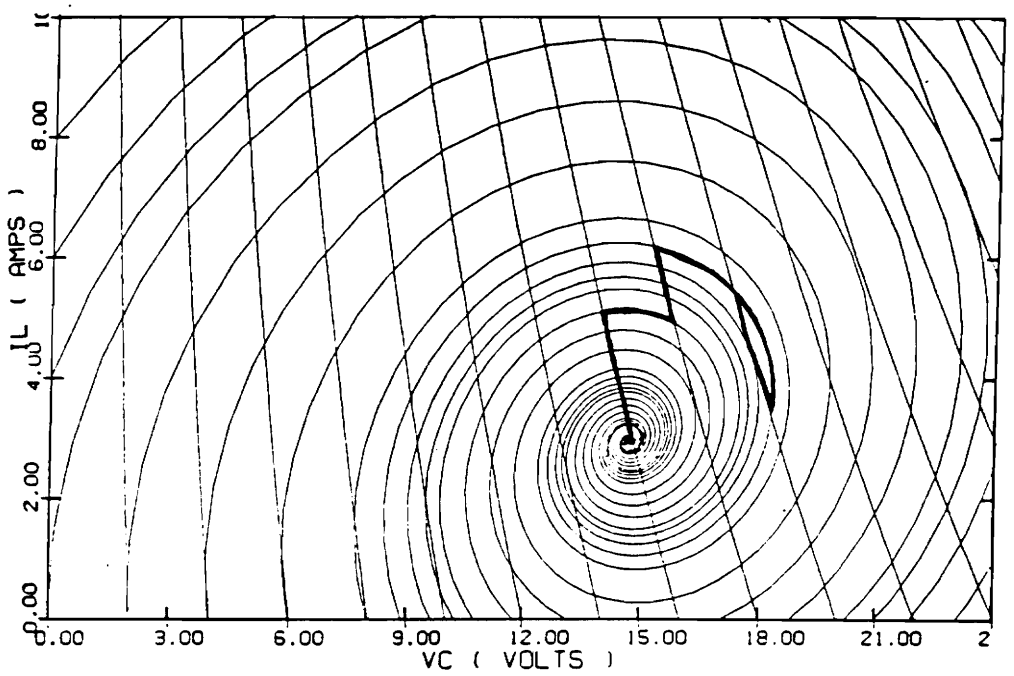

Figure 2.10 Phase plane portrait of boost converter and start-up trajectory

Three other start-up trajectories of a boost converter are shown in Fig. 2.11 with the assumption that the input voltage and transistor on-off command were applied at the same time. The start-up trajectory in Fig. 2.11 (a) assumes the converter begins its operation with transistor on command. Trajectory in Fig. 2.11 (b) illustrates the case the transistor off command is issued at the beginning of start-up process. As illustrated in those figures, both trajectories show a large excursion indicating the inductor current should go through the large value before it reachs a steady state. It is worthwhile to note that any transistor on command during the early stage of the start-up process will increase the peak value of the inductor current. The minimum value of the inductor current which any start-up trajectory must go through can be identified from the phase-plane portrait of converter. The start-up trajectory of boost converter, which has a minimum excursion of inductor current, is shown in Fig. 2.11 (c) with the assumption that the converter holds the off-time subcircuit during the early stage of start-up process.

In Fig. 2.12, a simplified trajectory of buck/boost converter is shown on the converter's phase-plane portrait which is composed of phase-plane portraits of subcircuit A and subcircuit C. Steady state trajectory is represented by a closed path in phase-plane as before. The start-up trajectory may reach to the steady state trajectory. without undergoing a large excursion.

Above examples show how phase-plane portraits of subcircuits can be used to predict the general behaviour of transient trajectory of converters. The simplified start-up trajectories shown in this section are rather artificial and may be different from the real start-up trajectories of the converters when other nonlinearities such as soft start circuit, duty ratio limitation and current limiting are included. Neverthe-

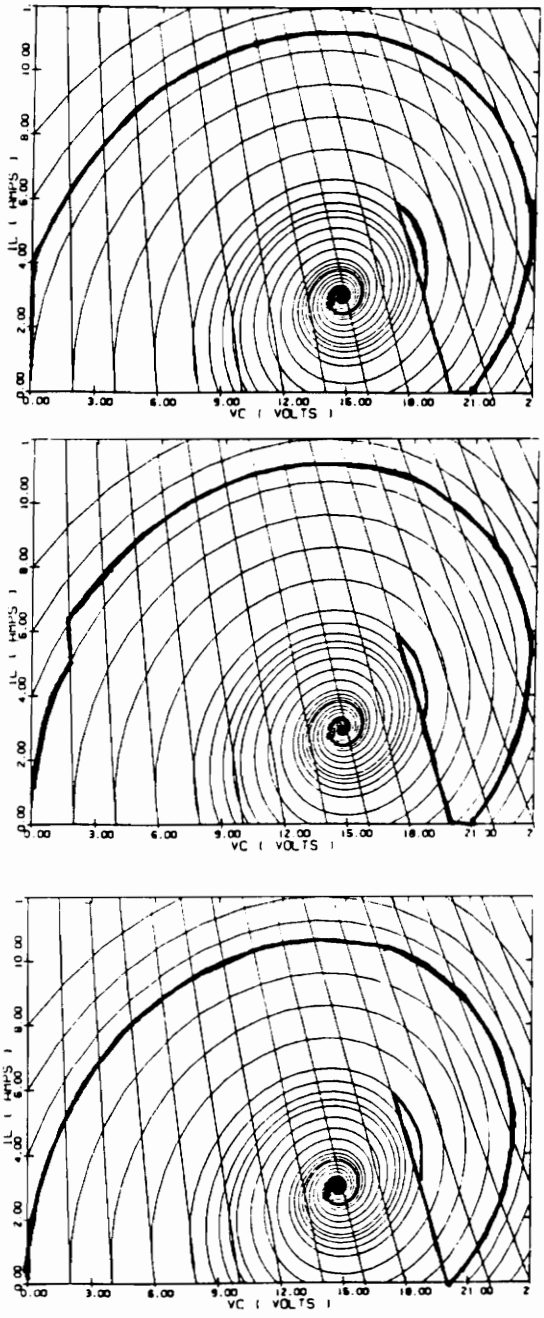

Figure 2.11 Phase plane portrait of boost converter and start-up trajectories
(a) Start-up with ON command (b) Start-up with OFF command
(c) Trajectory with minimum current excursion

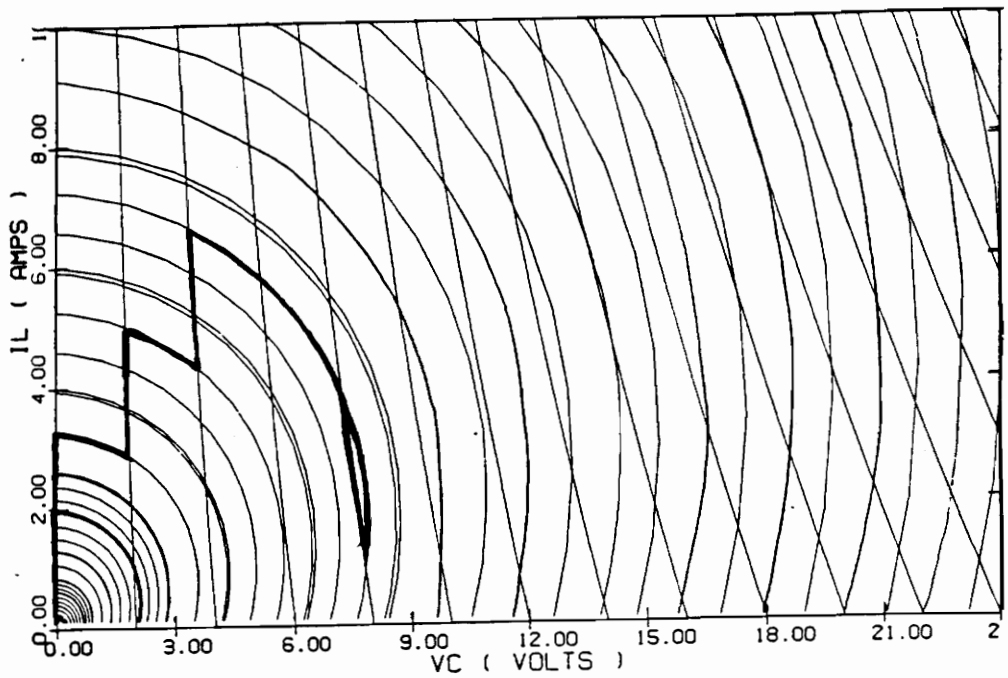

Figure 2.12 Phase plane portrait of buck/boost converter and start-up trajectory

less, they provide a picture of start-up mechanism and large-signal behaviour of the converters. A more realistic start-up trajectory will be introduced in Chapter IV.

Several interesting observations can be made from the phase-plane portraits of the converters in Fig. 2.13. First, the phase-plane portrait of the buck converter has two stable spiral points. On the other hand, the boost and the buck/boost converter's phase-plane portraits have a stable spiral point and a stable node. Their structures are almost the same except the location of equilibrium point. As a result, the boost and the buck/boost converter have very similar transient trajectories as we will see later.

Secondly, whereas the phase-plane portraits of off-time subcircuit of buck and the buck/boost converters have equilibrium points at the origin, neither of the boost converter's subcircuit has the equilibrium at the origin. Furthermore, the boost the converter's phase-plane portrait shows the existence of an unavoidable large excursion of inductor current in start-up process. The above observation have a simple physical interpretation. In the buck or the buck/boost converter the transistor is connected to the input voltage in series. Thus, the inductor current can be controlled within a certain bound by transistor on-off commands during start-up. However, in the boost converter, the inductor is directly connected to the input voltage. As a result, the inductor current will increase regardless of the transistor on-off command at the early stage of start-up as illustrated in Fig. 2.11.

Finally, the phase-plane portraits provide some insight about the steady state voltage gain of the converters. For the stable steady state operation, the trajectory must have a closed path within a fixed switching period. From the phase-plane portrait of the buck the converter, it is obvious that any closed path trajectory can be found only in

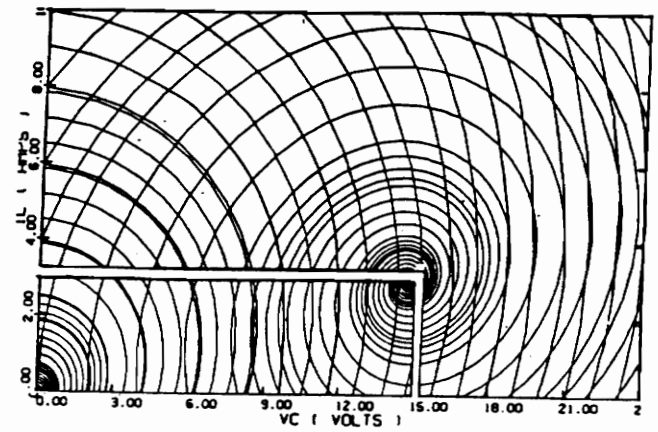

(a) Buck converter

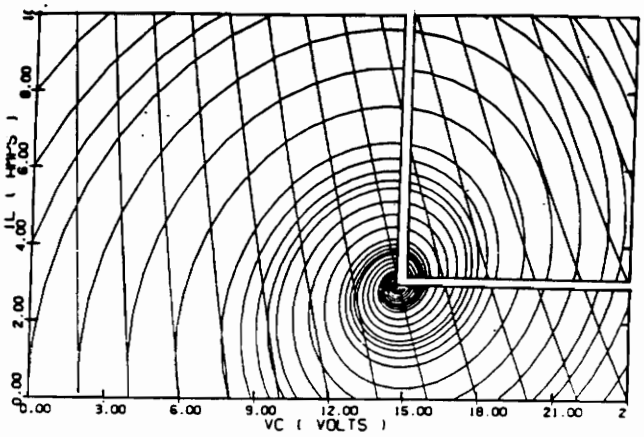

(b) Boost Converter

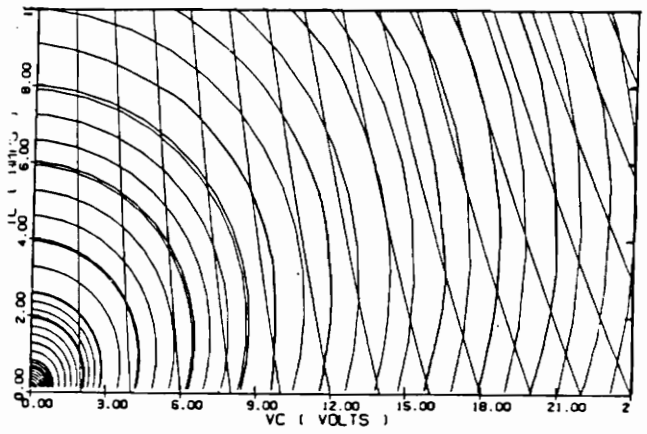

(c) Buck/boost Converter

Figure 2.13 Phase plane portrait of converters
(a) Buck converter (b) Boost Converter
(c) Buck/boost Converter

lower left hand region (shown separated by the double lines) in Fig. 2.13(a). Thus, the voltage gain of the buck the converter is always less than unity. Similarly, for the boost converter, any closed path trajectory can be found only in upper right hand region (shown separated by the double lines) in Fig. 2.13 (b) which accounts that the voltage gain of the boost converter is always greater than unity

2.5 Conclusion

The graphical phase-plane method was employed to study the qualitative behaviour of the buck, boost and the buck/boost converters.

To explain the behaviour of the converter systematically, the structure of each converter was investigated and four subcircuits which represent these converters precisely depending on the state of switches were introduced. Using the inductor current and capacitor voltage as two coordinates of phase-plane, the phase-plane portrait of each subcircuit was explained.

The phase-plane portrait of each converter was obtained by overplotting the phase-plane portrait of its subcircuits. A simplified start-up trajectory of each converter was explained providing a considerable insight into the transient behaviour of converter. The phase-plane portraits of three basic the converters are compared.

III. GLOBAL BEHAVIOUR OF STATE TRAJECTORIES

3.1 Introduction

The large signal transient trajectories of converters is discussed in the phase plane. A number of new ideas are employed to describe the transient behaviour of converters.

In Section 3.2, the converter control schemes, whose characteristics dominate the transient response of converters, are reviewed briefly. The steady state trajectory of a converter is introduced in Section 3.3. The envelopes of steady state trajectories are explained by considering a family of trajectories with different steady state duty ratios. As we will see later, those envelopes provide many information about the transient behaviour of a converter. The equations of these envelopes are presented with assumptions.

In Section 3.4, several terminologies are introduced to characterize the transient trajectories. Computer generated trajectories are interpreted in terms of them. A transition pattern of arbitrary trajectory is given in this section also.

3.2 Controller of DC-to-DC Converter

The controller generates a sequence of the transistor on-off commands according to the control law during converter's operation. The particular sequence of on-off commands, which entirely depends on the characteristics of controller, governs the transient response of converter. Therefore, the transient response of a converter mainly depends on the characteristics of controller in addition to circuit parameters. With the same initial condition and same circuit parameters, the converter may have different transient trajectories by virtue of different control schemes.

There are several types of controllers such as **constant frequency, constant on-time, constant off-time,** and **free running** types. Throughout this thesis, the converters are assumed to be operated by the constant frequency type controllers which are characterized by a fixed switching period with a variable ratio of transistor on-time to switching period. The variable ratio, which is called the **duty ratio,** plays an important role in the transient behaviour of the converter. In the converter with constant frequency type controller, the ultimate function of the controller is to change the duty ratio within a fixed switching period and the converter is called the **duty ratio controlled converter** in this sense.

In the duty ratio controlled converter, the transient response is the portion of operation where the controller is adjusting the duty ratio continuously in an attempt to arrive at a steady state. On the other hand, the steady state response is the portion of operation where the controller provides a fixed duty ratio. Hence, the steady state operation of converter is characterized by its fixed duty ratio.

Two kinds of control strategies are widely used for the duty ratio controlled converters. The first method known as the **single-loop control** uses the output voltage and an external ramp function to generate the duty ratio control signal. The output voltage is compared with a fixed reference voltage to yield the error voltage. The error voltage is connected to the input of a differential amplifier with suitable compensation circuitry to optimize the small signal characteristics of converter. Finally, the output of a differential amplifier is compared with the external ramp to generate the pulse width modulated duty ratio control signal as shown in Fig. 3.1 (a).

The other method, which is called the **two-loop control** , utilizes both output voltage and inductor current or switch current to produce duty ratio control signal. Sensing the switch current, which is called current-mode control, is widely used due to several advantages over using an inductor such as inherent over-current protection and current sharing in parallel module converters. It also provides the same advantages of two-loop control as in the inductor current sensing scheme. Thus, for two-loop control, the current-mode control will be discussed in this thesis and the terminologies 'two-loop control' and 'current-mode control' will be used interchangeably. The output voltage is compared with reference voltage as before. The resulting error signal is connected to the differential amplifier to yield voltage loop error signal. The switch current is multiplied by a constant gain to produce the current loop feedback

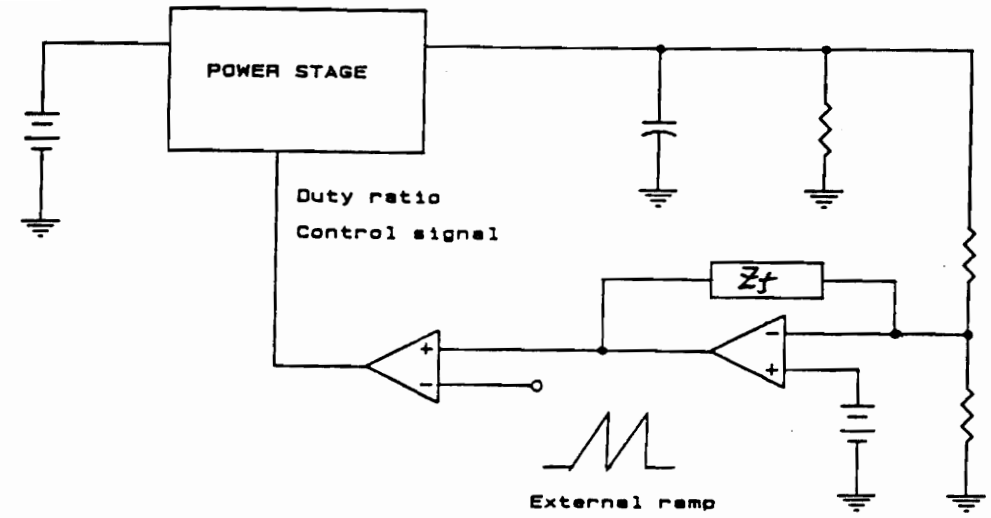

(a)

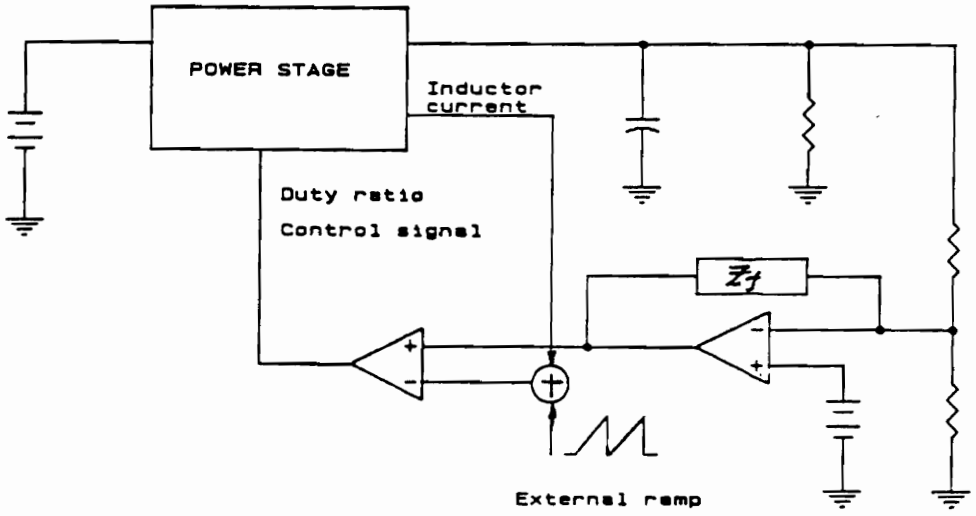

(b)

Figure 3.1 Control methods of duty ratio controlled converter
(a) Single loop control (b) Two loop control

voltage. The current loop feedback voltage is added with an external ramp function and compared with voltage loop feedback voltage to generate the duty ratio control signal as shown in Fig. 3.1 (b).

3.3 Steady State Trajectories and Envelopes

The converter starting from the arbitrary initial condition goes through some transient and eventually reaches the steady state by virtue of feedback controller. Unlike other linear systems, the trajectory of the converter in a steady state is a closed path and the time domain waveforms of the state are periodic with the non-zero ripple components. The shape, size and location of the closed loop uniquely are determined by the set of circuit parameters and the switching period. The closed path determined by circuit parameters provides the steady state information about the converter.

The typical inductor current and capacitor voltage of a buck converter at a steady state with a constant frequency type controller are shown in Fig. 3.2(a) and (b). In Fig. 3.2(c), the corresponding state trajectory is also depicted. The on-time and off-time trajectory start at the same point for every transistor on-off cycle. The ending point of on-time trajectory is the starting point of off-time trajectory; conversely, the ending point of off-time trajectory is the starting point of on-time trajectory. It is important to note that these two points are uniquely determined by the duty ratio, circuit parameters and switching frequency.

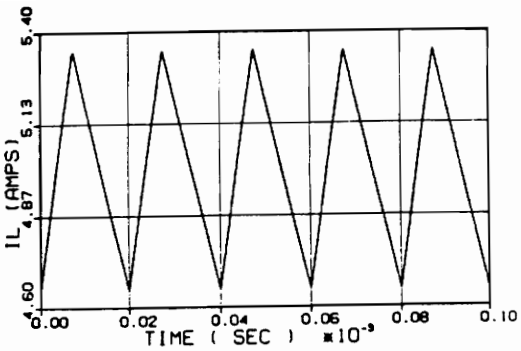

(a)

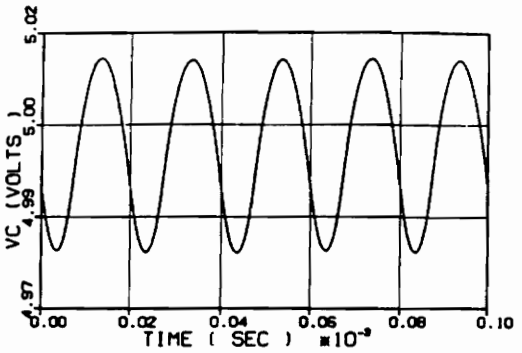

(b)

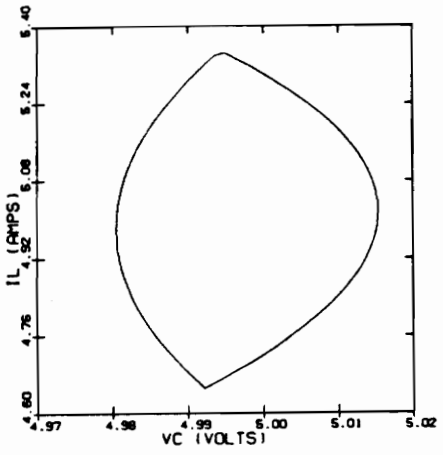

(c)

Figure 3.2 Steady state response of buck converter
(a) Inductor current (b) Capacitor voltage
(c) Trajectory

The highest and the lowest point of the closed path show us the maximum and minimum of inducter current, respectively. And the vertical distance between these points represents the peak-to-peak value of the inductor current ripple. Similarly, we can figure out the maximum and minimum value of the capacitor voltage and the peak-to-peak value of ripple component from the location of the furtherest right and left points of the closed path.

One of the most important functions of a controller is to regulate the capacitor voltage, which is the output of a converter, at a preset level by adjusting the duty ratio. Depending upon the desired output voltage, the converter may have the different duty ratio and different trajectory in steady state. However, once output voltage is specified, the converter with given circuit parameters has a fixed duty ratio and unique trajectory in steady state. Thus, there is a one to one correspondence between duty ratio and steady state trajectory of converter.

Fig. 3.3 shows a family of steady state trajectories of buck converter with different steady state duty ratios. Each closed path represents a steady state trajectory corresponding to the particular duty ratio. If we connect the highest point and the lowest point of closed paths, two curves will result as shown in Fig. 3.3. These curves are referred to as the **upper envelope** and the **lower envelope** of steady state trajectories. The upper and lower envelopes constitute the region in the phase plane where any steady state trajectory can exist. In other words, the steady state trajectory of a converter, whatever its duty ratio may be, should be located only in the region confined by these envelopes. As we will see later, these envelopes provide considerable information about the transient response of converter.

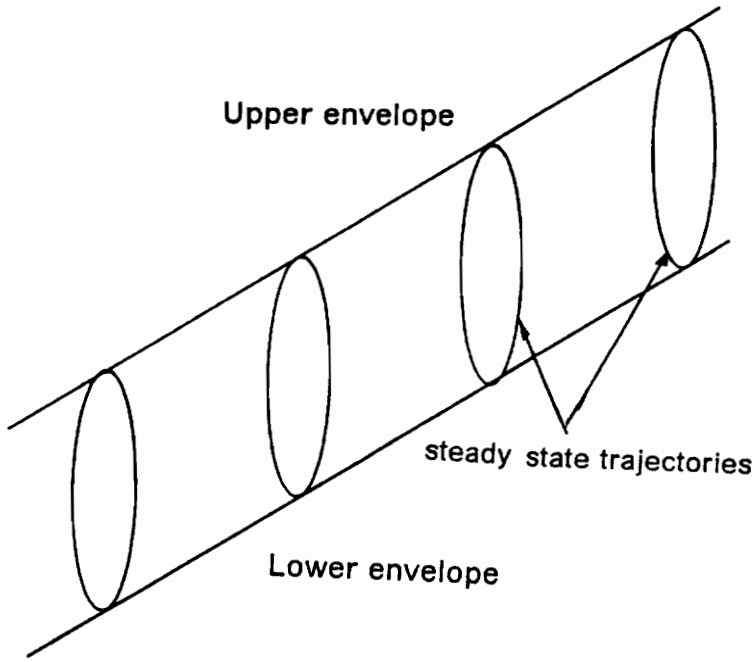

Figure 3.3 Steady state trajectories and envelopes of buck converter

The equations of the upper and lower envelopes for buck, boost and buck/boost converters are driven in the Appendix B with following assumptions.

- Parasitic resistance of the inductor can be neglected.
- The converter is operating in the continuous conduction mode.
- Inductor current can be approximated by a triangular wave.
- Capacitor voltage is constant.

BUCK CONVERTER

UPPER ENVELOPE :

$$I_{upper} = \frac{V_C}{2L}\left(1-\frac{V_C}{V_g}\right)Ts + \frac{V_C}{R}$$

LOWER ENVELOPE :

$$I_{lower} = -\frac{V_C}{2L}\left(1-\frac{V_C}{V_g}\right)Ts + \frac{V_C}{R}$$

where V_C : Capacitor voltage
V_g : Input voltage
Ts : Switching period
L : Inductor
R : Load resistor

BOOST CONVERTER

UPPER ENVELOPE :

$$I_{upper} = \frac{V_g}{2L}\left(1-\frac{V_g}{V_C}\right)Ts + \frac{V_C^2}{V_g R}$$

LOWER ENVELOPE :

$$I_{lower} = -\frac{V_g}{2L}\left(1 - \frac{V_g}{V_C}\right) Ts + \frac{V_C^2}{V_g R}$$

BUCK/BOOST CONVERTER

UPPER ENVELOPE :

$$I_{upper} = \frac{V_g}{2L}\frac{V_C}{(V_g + V_C)} Ts + \frac{V_C(V_g + V_C)}{V_g R}$$

LOWER ENVELOPE :

$$I_{lower} = -\frac{V_g}{2L}\frac{V_C}{(V_g + V_C)} Ts + \frac{V_C(V_g + V_C)}{V_g R}$$

The envelopes of steady state trajectories of buck, boost and buck/boost converters are overplotted on the phase-plane portraits given in the Chapter II in the Fig. 3.4.

The envelopes and the actual steady state trajectories of a buck converter operating at 50 kHz with different duty ratios are shown in Fig. 3.5. The circuit parameters of buck converter are repeated below for convenience.

Vg = 15 V

L = 100 μH

C = 50 μF

R = 5 Ω

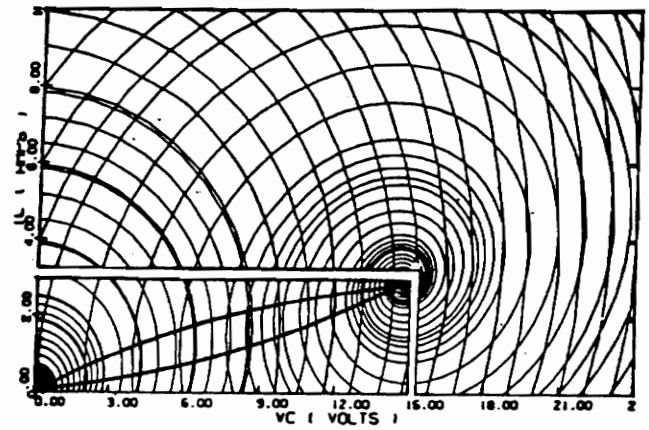

(a) Buck converter

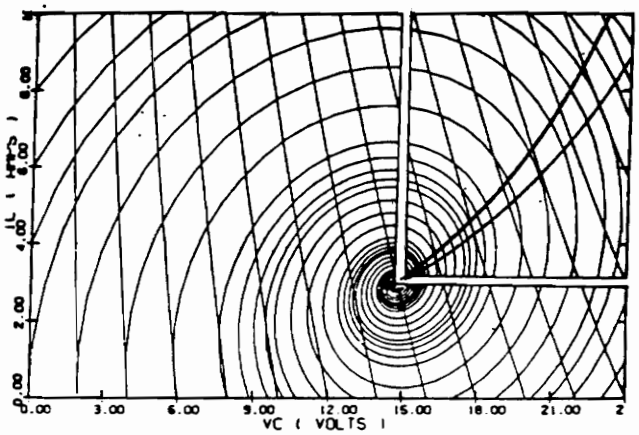

(b) Boost Converter

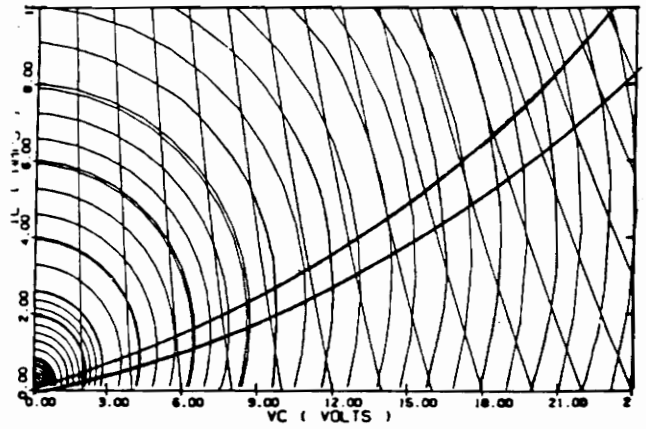

(c) Buck/boost Converter

Figure 3.4 Envelopes and phase plane portraits
(a) Buck converter (b) Boost converter
(c) Buck/boost converter

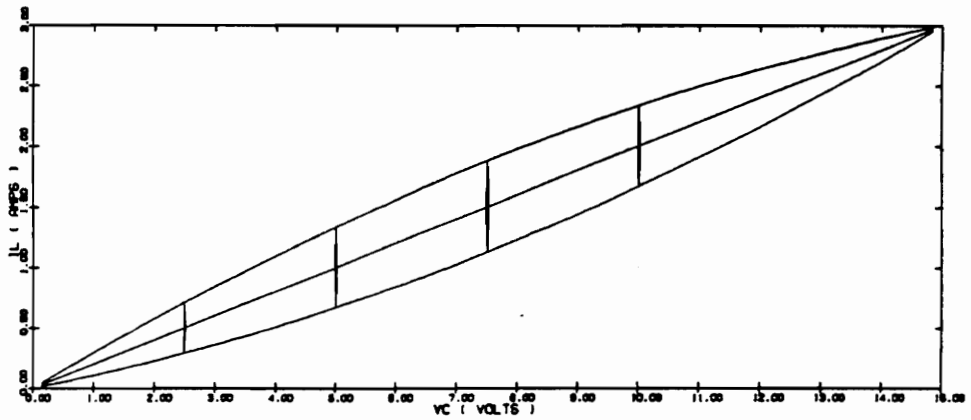

Figure 3.5 Steady state trajectory of buck converter
(Vg = 15V , L = 100μH , R = 5Ω , C = 50μF)

For boost converters, the envelopes and actual trajectories of each converter are plotted assuming the same switching period and circuit parameters as the buck converter case in Fig. 3.6. One of the assumptions used to derive the equations of envelopes is that the capacitor voltage is assumed constant. However, this assumption is not quite satisfied with the capacitor used in this converter resulting in slanted trajectories. As a result, the envelopes driven with constant capacitor voltage assumption fail to bound the trajectories as shown in Fig. 3.6 (a). To avoid this situation, the capacitor is increased to 500 μF making the constant capacitor voltage assumption as a satisfactory one. Since the most important design consideration of a converter is to have a small capacitor voltage ripple, the constant capacitor voltage assumption is easily satisfied in practice. With a sufficiently large capacitor, the envelopes approximate the bounds of trajectories well. The trajectories look like straight lines with very little capacitor voltage ripples as shown in Fig. 3.6 (b).

The simulation result of steady state trajectories of the buck/boost converter are overplotted with the envelopes of trajectories as shown in Fig. 3.7. The trajectories of the converter with the same parameter values as a buck converter are shown in Fig. 3.7(a) and that of the converter with C = 500μF are given in Fig. 3.7(b). With the larger capacitor, the envelopes approximate the bounds of trajectories more accurately as expected.

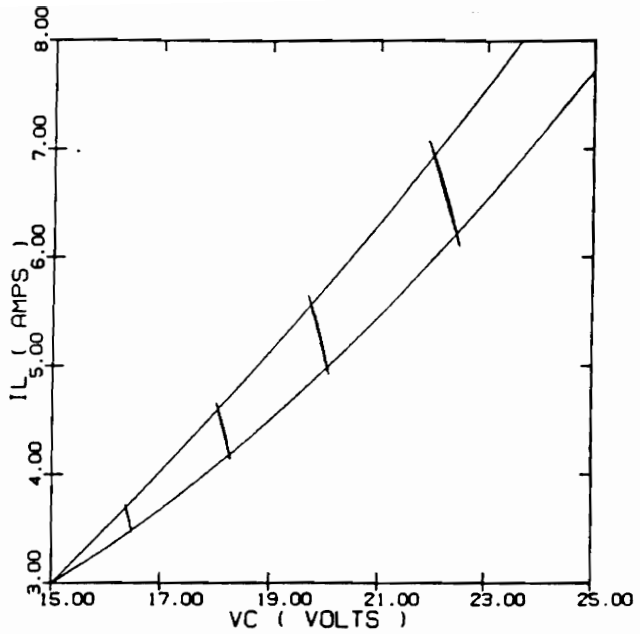

(a)

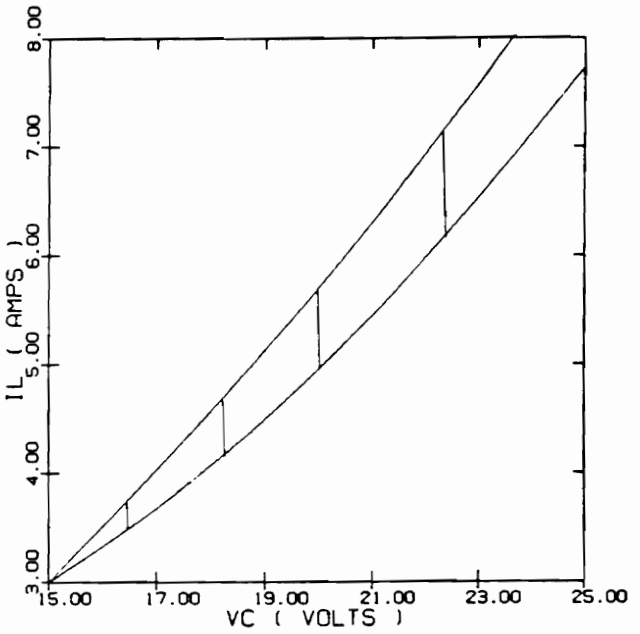

(b)

Figure 3.6 Steady state trajectories of boost converter
(a) Vg = 15V , L = 100μH , R = 5Ω , C = 50μF
(b) Vg = 15V , L = 100μH , R = 5Ω , C = 500μF

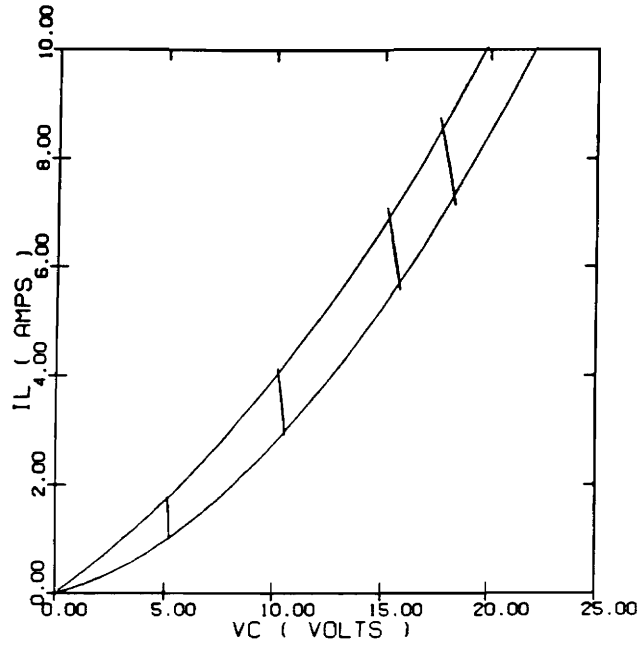

(a)

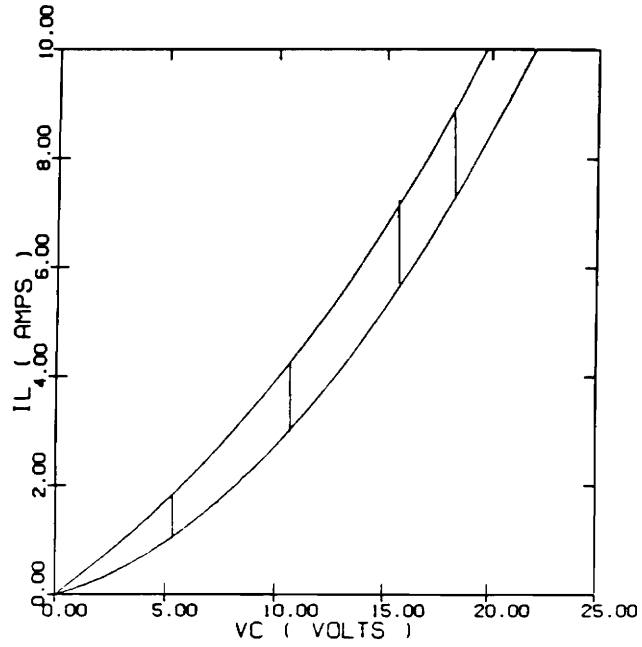

(b)

Figure 3.7 Steady state trajectories of buck/boost converter
(a) Vg = 15V , L = 100μH , R = 5Ω , C = 50μF
(b) Vg = 15V , L = 100μH , R = 5Ω , C = 500μF

3.4 Global Behaviour of Transient Trajectory

Whereas the phase-plane portrait of a converter provide information about the trajectory of converter, the dynamic properties of controller plays a dominant role in the transient response of converter. Converters having the same phase-plane portrait may show an entirely different transient trajectory by virtue of different characteristics of the controller.

In the duty ratio controlled converter, the transient response results directly from the change of duty ratio. Thus, the transient trajectory can be investigated in terms of the duty ratio variation. If the duty ratio is allowed to change over a wide range, the trajectory would go through a large transition. On the other hand, the trajectory would show a systematic behaviour with gradually changing duty ratio.

The transient trajectory of converter can be divided in the following three modes according to its behaviour and changing pattern of duty ratio.

- **Large transition mode** : The portion of trajectory which shows relatively large transient behaviour which can not characterized systematically. The change of duty ratio is usually large in this mode.

- **Duty ratio tuning-mode** : The portion of trajectory which shows a systematic behaviour. The change of duty ratio in this mode is small and continuous.

- **Steady state** : The portion of trajectory which travels a fixed closed path, namely, a steady state trajectory.

A typical transient trajectory undergoes the large transient mode and then starts duty ratio tuning-mode operation, eventually ending up with the steady state trajectory.

An example of transient trajectory of buck converter is shown in Fig. 3.8(a). The time domain waveforms of state (inductor current and capacitor voltage) and the duty ratio of each switching period are depicted in Fig. 3.8(b) and 3.8(c), respectively. The trajectory originated from the arbitrary initial state (marked by " X ") passes through the large transition mode. This mode corresponds to the first several switching cycles of time response in Fig. 3.8(b). The duty ratio in this mode changes in a large scale as shown in Fig. 3.8(c).

The duty ratio tuning-mode is the region of trajectory which shows a slow varying behaviour; that is trajectory is confined in some region and changing pattern of trajectory is quite systematic. Note that the capacitor voltage and inductor current change slowly and the duty ratio changes almost continuously in this mode. This mode ends up with steady state where the inductor current and capacitor voltage are periodic and the trajectory yields a steady state closed loop with a fixed duty ratio.

Before beginning the detailed discussion about each mode, we need to mention that although it is very difficult to predict converters' behaviour in large transition mode, the motion of trajectory in duty ratio tuning-mode can be predicted from circuit parameters, or, from phase-plane portrait.

LARGE TRANSITION MODE

The trajectory in this mode can be characterized by the relatively large scale transition with the large fluctuation of duty ratio. The duty ratio can be zero or one (which

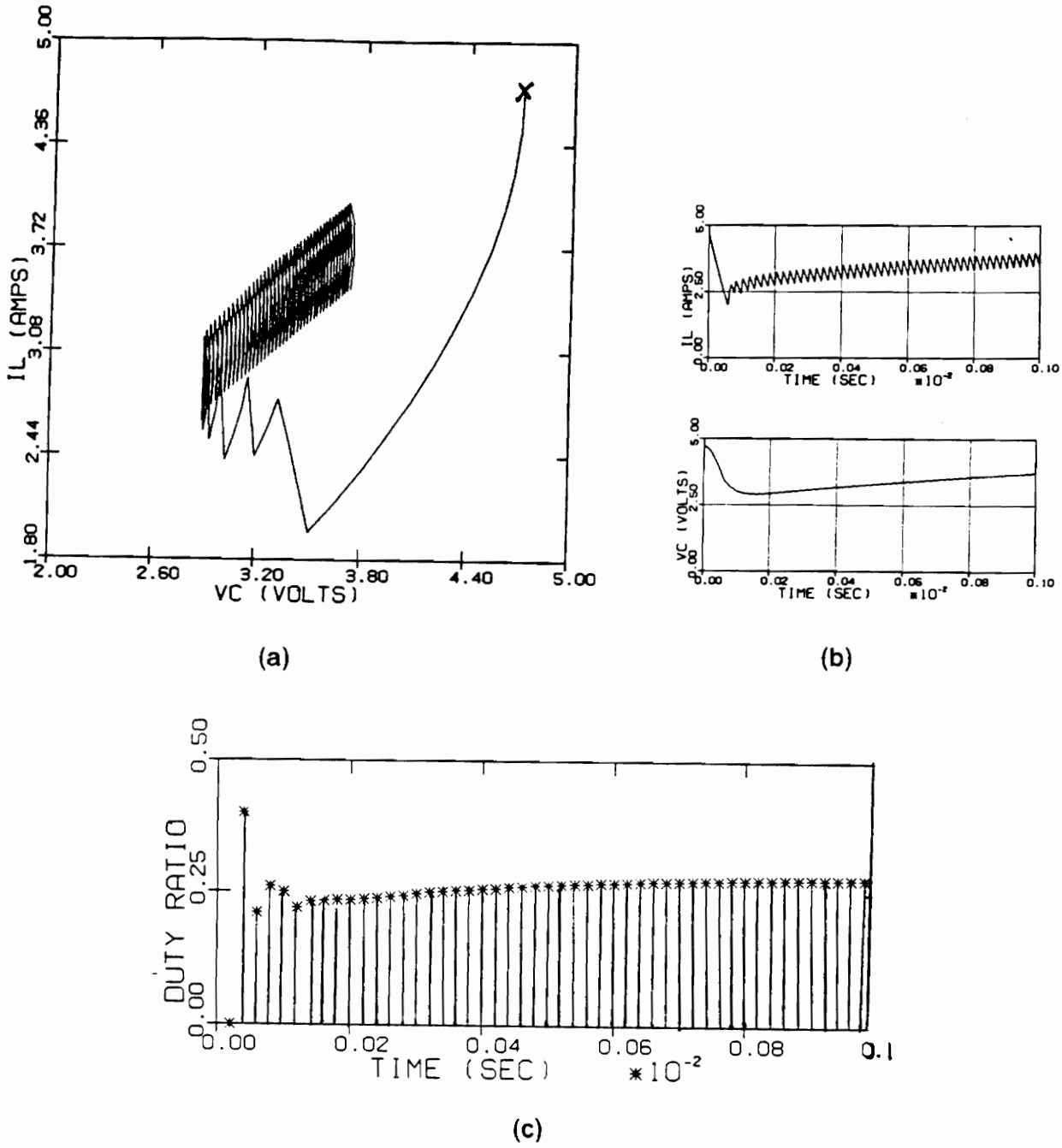

Figure 3.8 Transient response of buck converter
(a) Transient trajectory (b) Time response of state
(c) Duty ratio of converter

implies the converter stays in off-time or on-time subcircuit for a whole switching period) in this mode.

There are many factors from which the large transition mode of trajectory result. Some of them may be a large perturbation of state and nonlinearities in feedback controller. One typical large transition mode occurs in converter's start-up trajectory. At the early stage of start-up, the converter stays in on-time subcircuit or off-time subcircuit for several switching period. Also, various nonlinearities of the controller will affect the transition trajectory. The start-up trajectories of the converters will be discussed later in detail in Chapter IV.

DUTY RATIO TUNING MODE

The most prominent feature of this mode is that trajectory with gradual changing duty ratio can be characterized systematically. The typical trajectories of buck,boost and boost converters operating in this mode are shown in Fig. 3.9. As shown in this figure, the trajectories move in a regular fashion toward steady state. Although the detailed shape of the trajectory of converters are different, their moving patterns are quite similar. Furthermore, we will see that the moving pattern of each converter's trajectory can be predicted by its circuit parameters and operating conditions.

In this subsection, the behaviour of a trajectory in duty ratio tuning-mode will be explained with the buck converter example.

To understand the behaviour of a trajectory under duty ratio tuning-mode, consider the trajectories shown in Fig. 3.10. As explained in Section 3.3, there is a one-to-one relationship between duty ratio and steady state trajectory. The closed path in Fig.

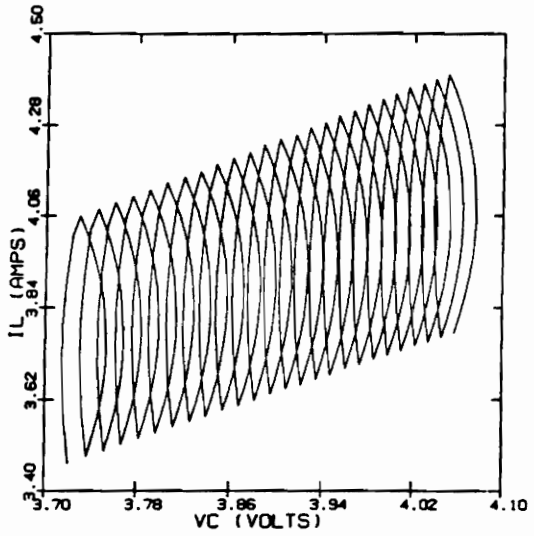

(a)

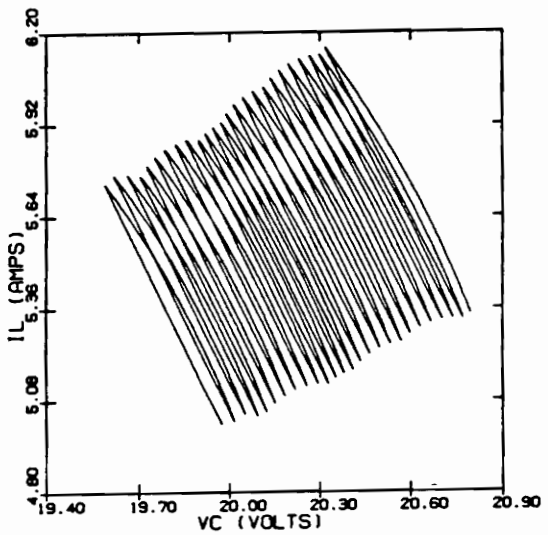

(b)

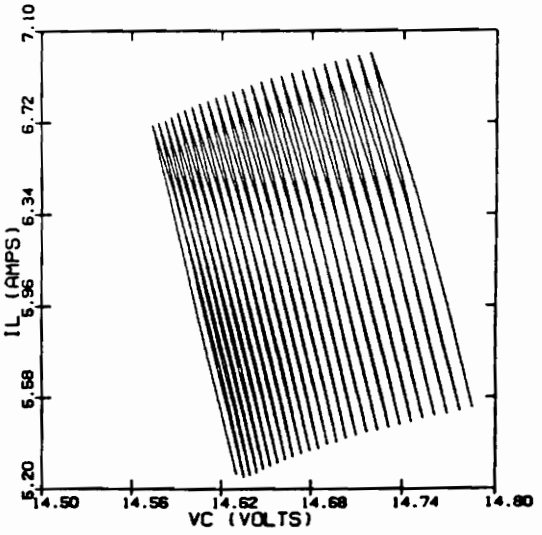

(c)

Figure 3.9 Trajectory in duty ratio tuning mode
(a) Buck converter (b) Boost converter
(c) Buck/boost converter

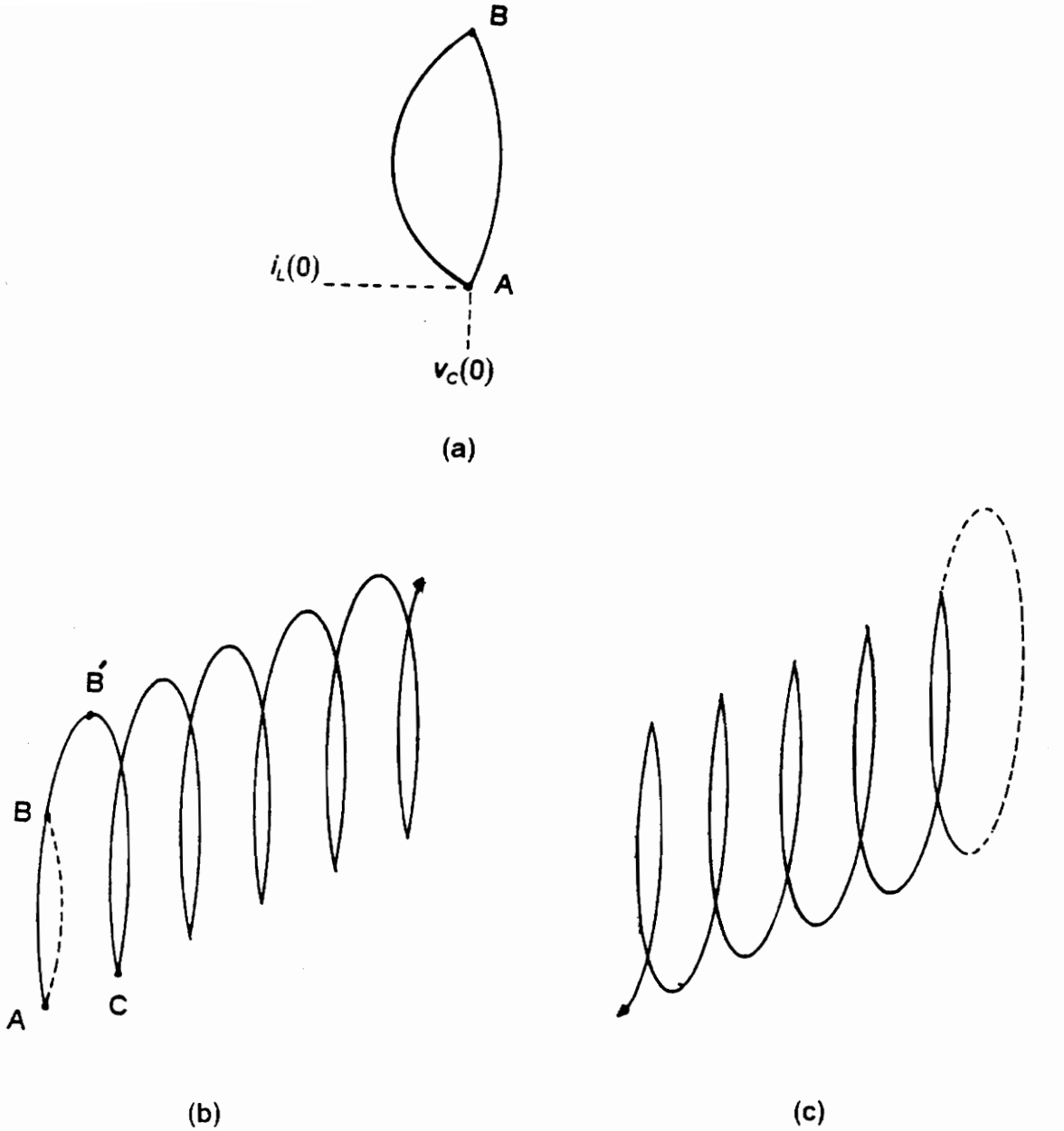

Figure 3.10 Trajectory of buck converter in duty ratio tuning mode
(a) Closed loop (b) Trajectory with increasing duty ratio
(c) Trajectory with decreasing duty ratio

3.10(a) represents the trajectory of a buck converter with a particular duty ratio D_1. Point A represents the place where transition from off-time subcircuit to on-time subcircuit takes place and point B represents the transition point from on-time subcircuit to off-time subcircuit. Obviously, the trajectory from A to B is a part of on-time trajectory and the curve from B to A is part of off-time trajectory.

If the converter starts its on-time operation with initial condition ($v_c(0)$, $i_L(0)$), the trajectory will trace out the trajectory shown in Fig. 3.10(a), provided that duty ratio is exactly D_1. A slightly different situation is explained in Fig. 3.10(b). The initial condition is the same as before, but the duty ratio is assumed to be larger than D_1. Additionally, it is also assumed that duty ratio increases in each consecutive switching period with the function of the controller. The time interval allowed for the converter to stay in on-time subcircuit is defined T_{ON}. Likewise, the time interval assigned to the off-time subcircuit is defined T_{OFF}.

$$T_{ON} = T_S\ D$$

$$T_{OFF} = T_S\ (1-D)$$

Where

T_S : Switching Period

D : Duty ratio

Initially, The trajectory travels the part of the arc from A to B as before. However, the increased T_{ON} prevents the trajectory from the following off-time trajectory at point B. As a result, the trajectory bypasses point B and starts to follow the off-time trajectory at the point B'. Since increasing T_{ON} implies decreasing T_{OFF} with a fixed switching period, point C, where the converter starts following on-time trajectory again, will be located somewhere above A as illustrated in Fig. 3.10(b). In the next switching pe-

riod, the on-time trajectory starting out at point C with further increased duty ratio will extend to point D. By continuing this procedure, the trajectory moves forward in a helical motion.

The transition trajectory with continuously decreasing duty ratio can be explained in a similar manner. Fig. 3.10(c) illustrates this situation. The closed path with broken line represents a trajectory generated by a fixed duty ratio and the solid line represents the trajectory of converter with a decreasing duty ratio. Note that the trajectory is moving backward in contrast to the motion of trajectory with increasing duty ratio.

There are many possible situations when the duty ratio tuning-mode takes place. The trajectories shown in Fig. 3.10 are only two simple cases. Nevertheless, the basic ideas used in the examples can be applied to the more case with appropriate modification. Consider the situation shown in Fig. 3.11. Again, the closed path with broken line stands for a closed path with a specific duty ratio D_1 and the coordinate ($v_C(0)$, $i_L(0)$) represent the instantaneous values of the state at the point A. Suppose that the converter initiates the on-time subcircuit operation with ($V_C(0)$, $I_L(0)$) and with duty ratio D_2 which is smaller than D_1. The controller is considered to provide the increasing duty ratios.

The trajectory originated at A goes through the on-time trajectory and it begins to follow off-time trajectory at point B' instead of B due to the smaller T_{ON}. The off-time trajectory is assumed to be effective up to the point C with larger T_{OFF}. We can think of another trajectory with duty ratio D_3 which starts on-time trajectory exactly at the point C. This trajectory is represented by a closed path with broken line near the point C. Note that that D_3 is smaller than D_1 since average capacitor voltage associated with the latter trajectory is smaller than that of the former trajectory and the

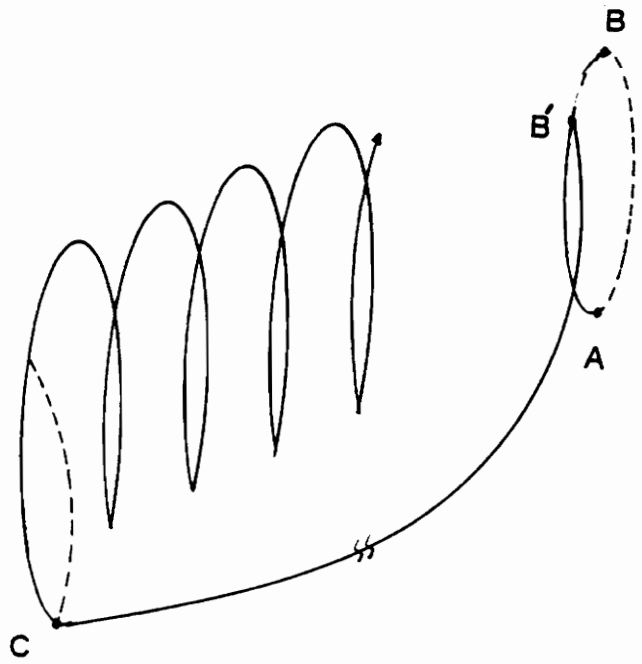

Figure 3.11 An example of trajectory of buck converter in duty ratio tuning mode

capacitor voltage of buck converter is proportional to duty ratio. The converter's new duty ratio when trajectory reaches C is assumed to be greater than D_3 by function of controller. At this point, the situation is exactly the same as the one considered in Fig. 3.10(b). By making use of the same argument used in that figure, the final trajectory is portraied in Fig. 3.11.

One important point to mention is that the trajectory in the duty ratio tuning-mode does not show any large deviation in moving pattern. Once the trajectory starts the duty ratio tuning-mode, it continues the same pattern as long as duty ratio changes gradually. This distinct feature of trajectory is used to identify the duty ratio tuning-mode.

To start the duty ratio tuning-mode operation, the converter should satisfy another condition in addition to the small variation of duty ratio between each consecutive switching periods. Fig. 3.12 shows a transient trajectory superimposed on the phase-plane portrait of buck converter. Whereas, the converter has almost constant duty ratio, the trajectory does not show the duty ratio tuning-mode. The reason for this is that the trajectory is located in the region where a closed path-like trajectory can not be made within a relatively small switching period. From the above example, we know that the converter trajectory should fall into some region to begin the duty ratio tuning-mode. In conclusion, the converter starts the duty ratio tuning-mode if following two conditions are satisfied.

- Initial state lies in the region where trajectory can form a closed path-like curve within predetermined switching period.

- Duty ratio is changing gradually.

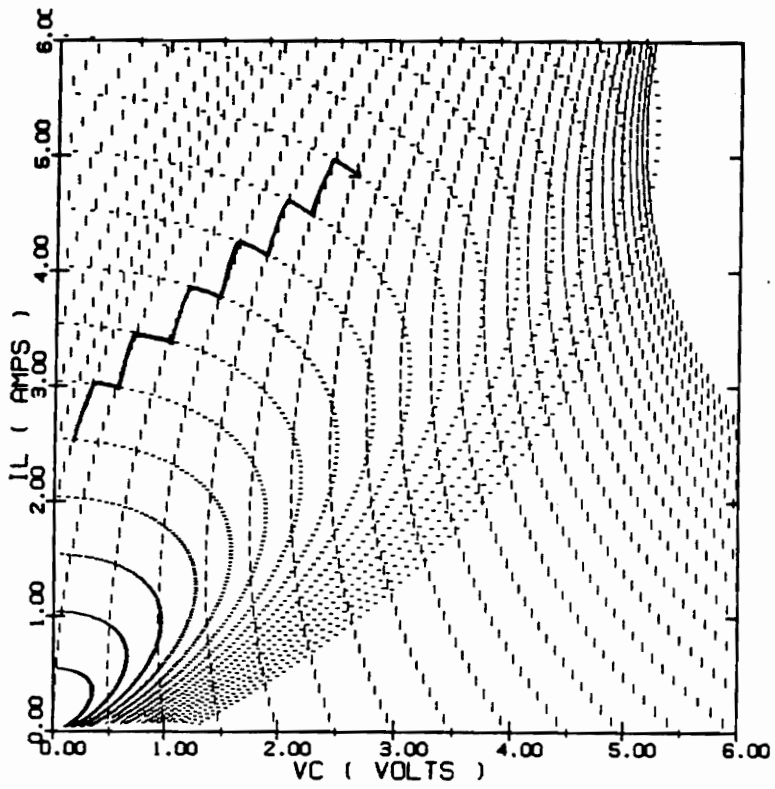

Figure 3.12 Transient trajectory of buck converter

In the Section 3.3, we introduced the upper and lower envelopes of steady state trajectories and derived their equations for buck,boost and buck/boost converters. The upper and lower envelopes constitute a region in which all possible trajectories of a converter with arbitrary duty ratios should be located. Since this region results from a family of closed path trajectories, the trajectory, with slowly changing duty ratio, moves in a closed path-like manner in the neighborhood of this region. The region obtained by connecting upper and lower envelope is called the **region bounded by envelopes** . If trajectory meet the region bounded by envelopes with gradually varying duty ratio, it will begin the duty ratio tuning-mode. Fig. 3.13 shows a transient trajectory and the region bounded by envelopes of a buck converter. After the large transition mode, the trajectory hits the region bounded by envelopes and begins the duty ratio tuning-mode operation.

Another important feature of trajectory in duty ratio tuning mode is the trajectory tends to converge to the region bounded by envelopes if the converter is stable. The trajectory of a converter with a very close duty ratios in two consecutive switching periods is illustrated in Fig. 3.14. Two closed paths in this figure represent trajectories with two different duty ratios D_1 and D_2. Two lines, $\overline{AB}$ and $\overline{CD}$, constitute the region bounded by envelopes. The trajectory of a converter with increasing duty ratio is depicted with broken line with the assumption that duty ratio of converter is taking the values between D_1 and D_2. Note that the trajectory of converter is, approximately, confined in the region bounded by envelopes. The smaller the variation of duty ratio becomes, the closer the region bounded by envelopes confines the trajectory. A simple extention of above reasoning explains the tendency of trajectory converging to the region bounded by envelopes.

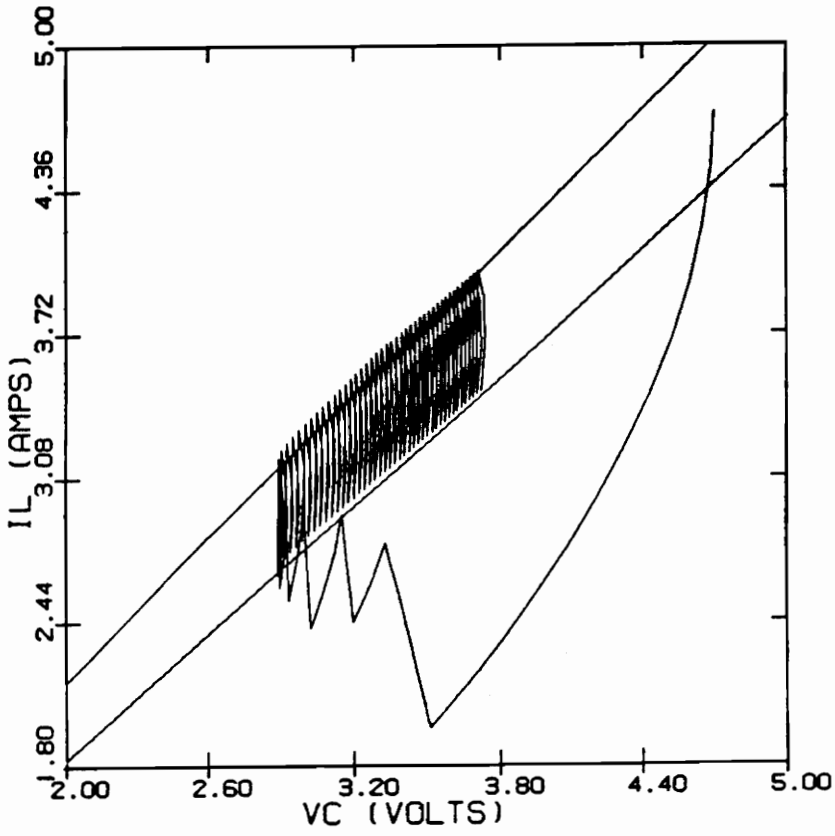

Figure 3.13 Transient trajectory and attraction region of buck converter

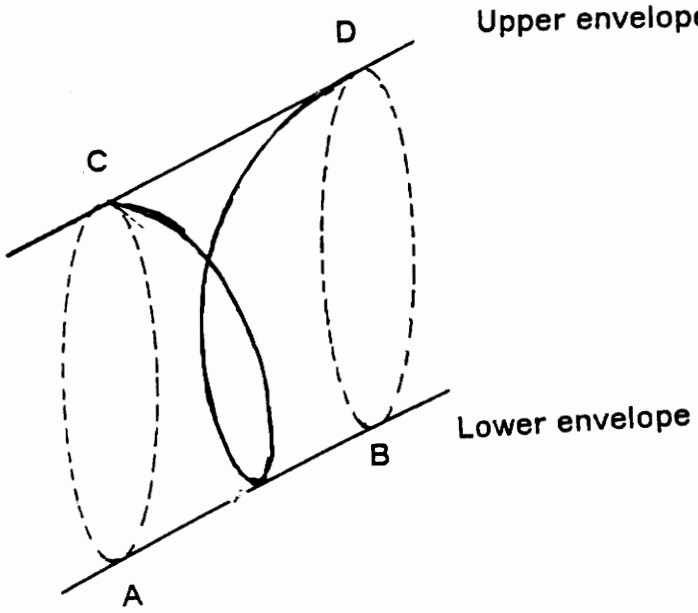

Figure 3.14 Trajectory of buck converter with very slowly changing duty ratio

As a conclusion, we can make a conclusion about the behaviour of trajectory in duty ratio tuning-mode. **With the duty ratio converging to the steady state duty ratio, the trajectory converges to the region bounded by envelopes.**

GLOBAL BEHAVIOUR OF TRANSIENT TRAJECTORY

For convenience, only a buck converter is considered in drawing the conclusion about the general behaviour of transient trajectory in the previous subsection. It should be noted, however, the validity of conceptual reasoning presented in that subsection is not dependent on the particular choice of converter model. Thus, the same argument is applied to boost and buck/boost converter.

The behaviour of the transient trajectory of converters is summerized below as a conclusion of this section.

- Trajectory undergoes the large transition mode with an arbitrary initial condition.
- The converter begins the duty ratio tuning-mode operation as trajectory approaches in the neighborhood of the region bounded by envelopes.
- The trajectory converges to the region bounded by envelopes in duty ratio tuning-mode.
- The trajectory forms a stable closed path in steady state.

The computer generated transient trajectories of the buck,boost and buck/boost converters are shown in Figs. 3.15, 3.16 and 3.17. The region bounded by envelopes

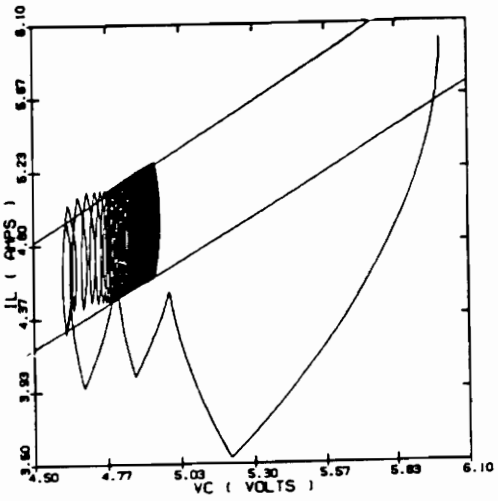

(a)

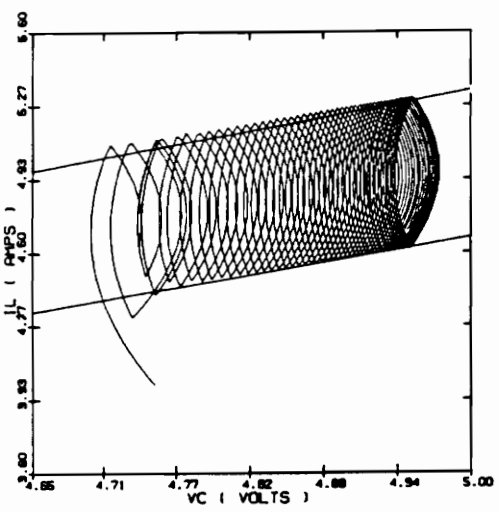

(b)

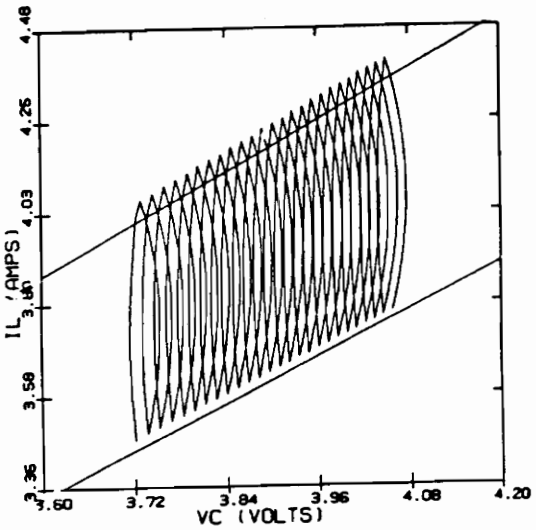

(c)

Figure 3.15 Transient trajectory of buck converter
(a) Large disturbance of state (b) Small disturbance of state
(c) Duty ratio tuning mode

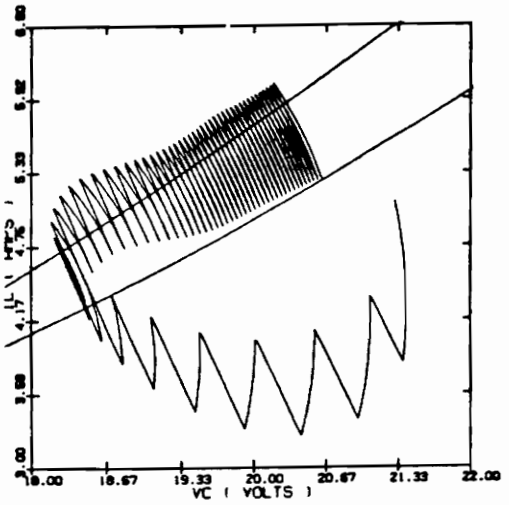

(a)

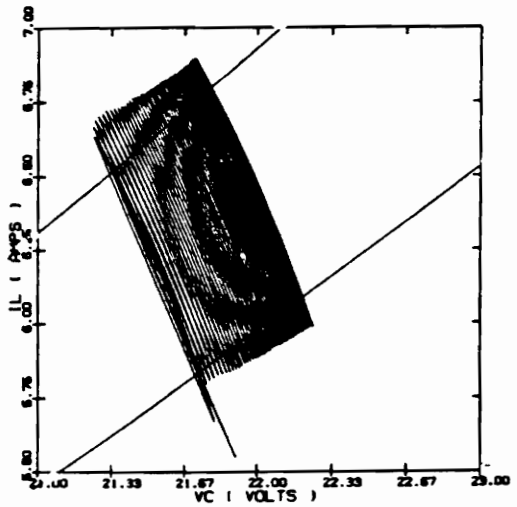

(b)

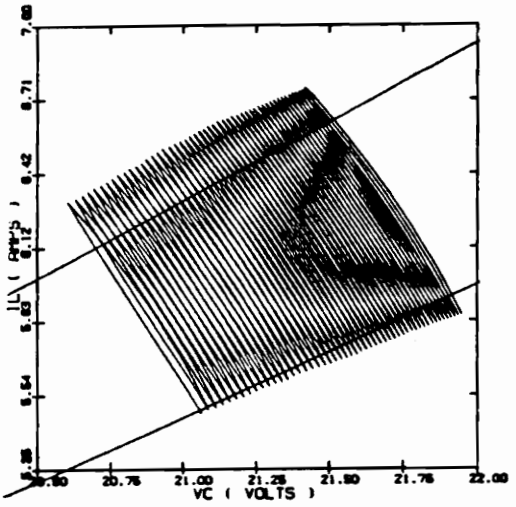

(c)

Figure 3.16 Transient trajectory of boost converter
(a) Large disturbance of state (b) Small disturbance of state
(c) Duty ratio tuning mode

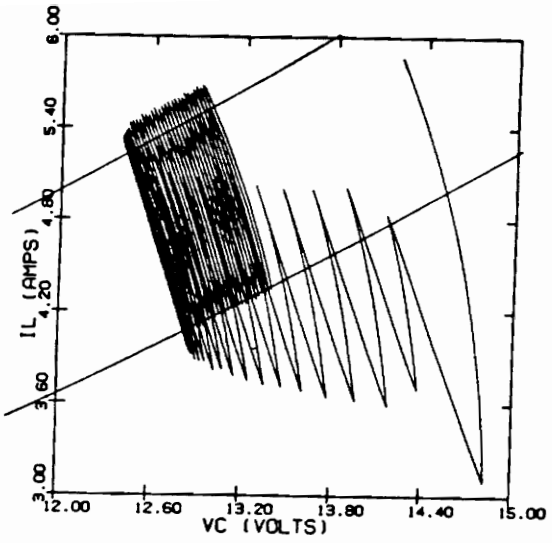

(a)

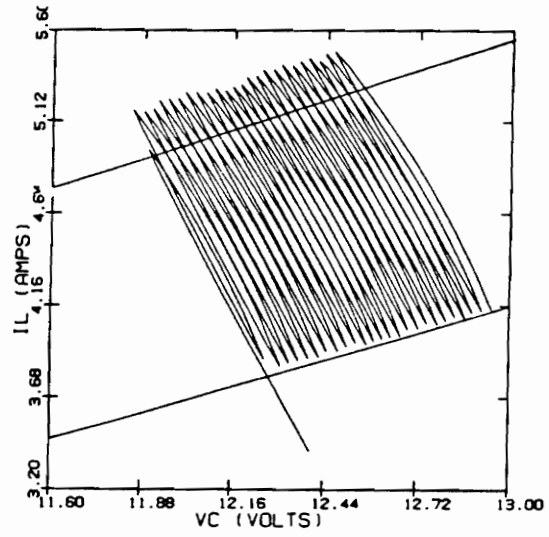

(b)

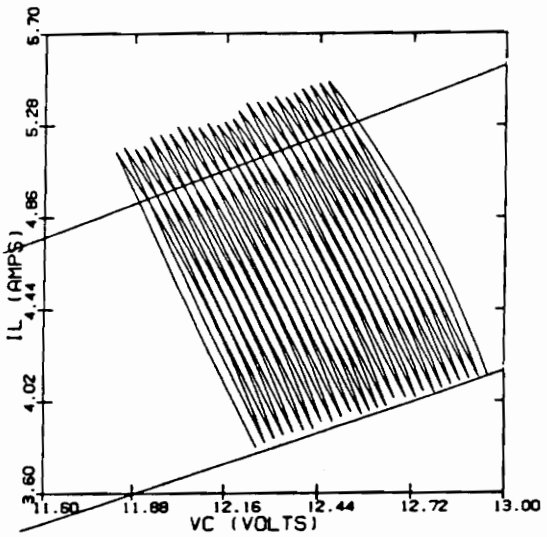

(c)

Figure 3.17 Transient trajectory of buck/boost converter
(a) Large disturbance of state (b) small disturbance of state
(c) Duty ratio tuning mode

TABLE 4-1

	Buck	Boost	Buck/boost
Vg	15 V	15 V	15 V
L	100 μH	100 μH	100 μH
C	50 μF	50 μF	50 μF
R	1 Ω	5 Ω	5 Ω
RI	0.1 Ω	0.1 Ω	0.1 Ω
T_s	20 μ sec	20 μ sec	20 μ sec

of these plots are found by making use of section 3.3 and the parameter values used in those simulation is listed in Table 4.1. For boost and buck/boost converters, some difference between envelopes and bounds of trajectory is resultant of the relatively small value of capacitor.

3.5 Conclusion

The transient trajectories were investigated in the phase-plane. With the aid of envelopes of steady state trajectories, the transient patterns of trajectories were presented. The steady state trajectory in the duty ratio controlled converter was discussed leading to the introduction of envelopes of them. The envelopes define the region in the phase-plane to which any stable trajectory will converge. This provides useful information about large signal properties of converter. We can predict the transient trajectory from them. Analytical expressions of envelopes of steady state trajectories are given.

The transient trajectory was divided into two modes according to the transition pattern in phase-plane. The large transition mode is characterized by relatively large variation of trajectory and the duty ratio tuning-mode is characterized by systematic behaviour of trajectory. The behaviour of trajectory in each mode was discussed in details focusing the relation between transition pattern and change of duty ratio. The region bounded by envelopes was introduced to define the region to which any stable transient trajectory converges. The behaviour of arbitrary transient trajectories was

given in terms of large transition mode and duty ratio tuning mode in conjunction with the region bounded by envelopes.

IV. LARGE SIGNAL TRANSIENT TRAJECTORY

4.1 Introduction

In this chapter, the large signal transient trajectories of buck,boost and buck/boost converters are analyzed. The computer generated transient trajectories are interpreted in terms of concepts introduced in Chapter III. The qualitative behaviour of trajectories of practical interest is explained

The start-up trajectory is presented in Section 4.2. As discussed before, the boost converter may have two start-up situations depending on the initial condition. In Section 4.3, the step-load change trajectories are investigated focusing on the behaviour of capacitor voltage. The input voltage change trajectories are studied in Section 4.4 in a similar way to the step-load change response.

If there is no explicit comment, the circuit parameters used in Section 3.4 are assumed and the current mode controller is used throughout this chapter.

4.2 Start-up Trajectory

One of the largest transients of a converter may be the start up process. The behaviour of start-up trajectories of converters are discussed in this section. The behaviour of them is explained on the basis of concepts introduced in previous chapter. Nonlinearities such as soft start circuit, duty ratio limitation and pulse-by-pulse current limiting will not be considered in this section.

Buck Converter The start-up trajectories of buck converter are shown in the Fig. 4.1 on the phase-plane portrait. The single-loop controller is used to generate the first trajectory. and current-mode controller is employed to the second trajectory. As shown in this figure, the two different controllers result in different trajectories on the same phase-plane portrait. The basic difference between the controllers discussed in the Chapter III, (the single loop controller uses only output voltage and the two-loop controller uses both output voltage and switch current to determine the duty ratio), is responsible for noticeablly unlike transition pattern of trajectories. Even though two trajectories look different, they have a common transition pattern. In Fig. 4.2, the previous trajectories and envelopes of steady state trajectories are overplotted to show transition pattern more clearly. With the zero initial condition of power stage and feedback controller, the feedback control circuit generates the switch on command. Then, the controller will generate a series of switch on-off commands according to the state of converter and feedback control law. At the beginning of start-up, trajectories undergo the large transition mode by large excursion of duty ratio as explained in Section 3.4. Once the trajectories hit the region bounded by envelopes, they start the duty ratio tuning-mode. As Fig. 4.1 shows, the converter

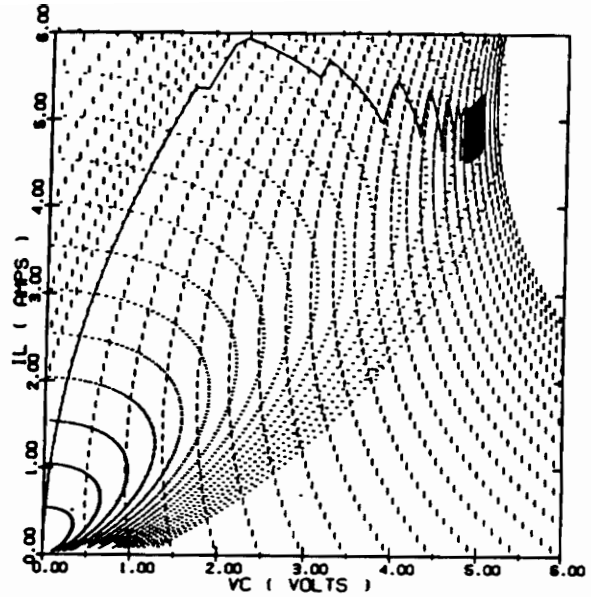

(a)

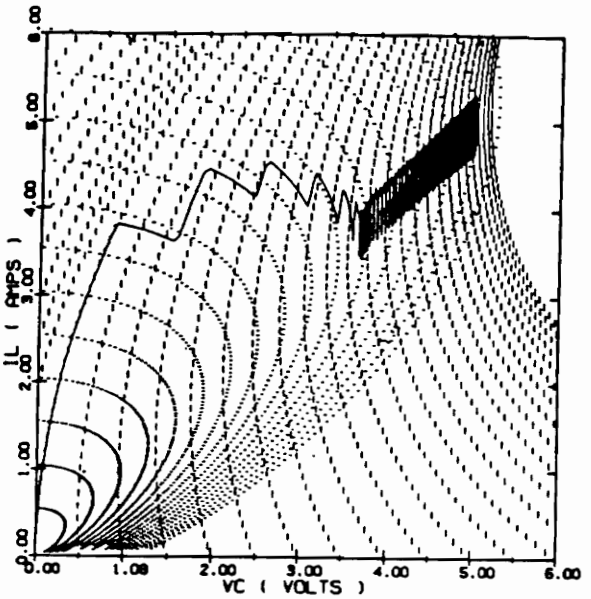

(b)

Figure 4.1 Start-up trajectories of buck converter
(a) Single loop control
(b) Two loop control

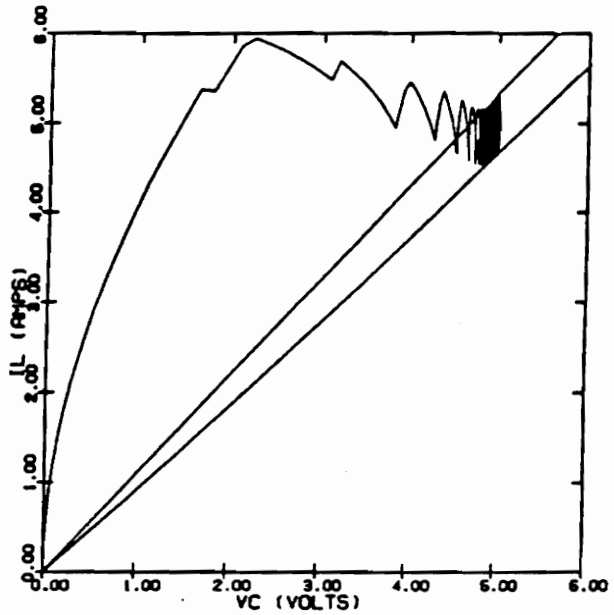

(a)

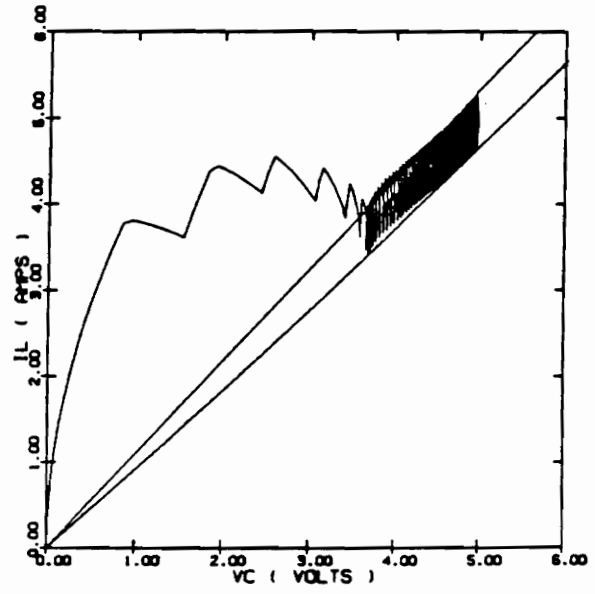

(b)

Figure 4.2 Start-up trajectories of buck converter
(a) Single loop control
(b) Two loop control

using the current-mode control reaches the duty ratio tuning-mode earlier and,thus, less inductor current excursion. This is because in current-mode control, the switch current is used together with the output voltage feedback to generate duty ratio control signal. The early switching action before the duty ratio tuning-mode is due to the dynamics in feedback compensation network.

Boost converter In the Fig. 4.3, two start-up trajectories of boost converters are depicted. The two-loop controller is employed to generated both trajectories. Since, for boost and buck/boost converters, it is not easy to achieve the optimum small-signal characteristics using a single-loop control, the two-loop control is widely employed in practice. The starting point of the first trajectory is the origin. The starting point of the second trajectory is the equilibrium point of subcircuit B in Fig. 2.4. In this case, it is assumed that the input voltage is applied earler than the switch on-off command. Thus, the converter has been held the subcircuit B. Note that the first trajectory shows a large excursion of inductor current as explained before. Due to the large excursion of inductor current which may saturates the core, it is clear that a soft start circuit is needed for the boost converter. This problem is even more severe in single-loop control in which the switch off command cannot be generated due to the large initial output error. The second trajectory originating from the equilibrium of subcircuit B shows more systematic behaviour. The start-up trajectories can be divided into a large transition mode and a duty ratio tuning-mode as before. The behaviour of trajectories can be explained in the same way as the buck converter case. Fig. 4.3 shows the start-up trajectories and region bounded by envelopes. Again, the trajectories converges to the region bounded by envelopes as time increases.

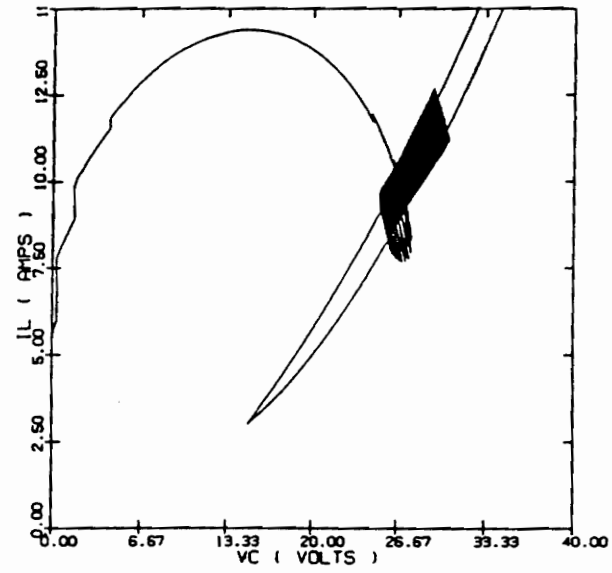

(a)

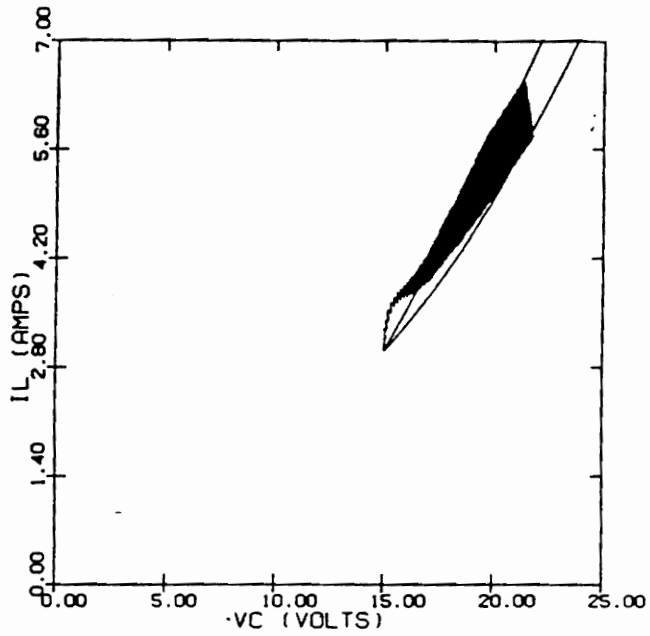

(b)

Figure 4.3 Start-up trajectories of boost converter
(a) Starting from origin
(b) Starting from equilibrium point of subcircuit B

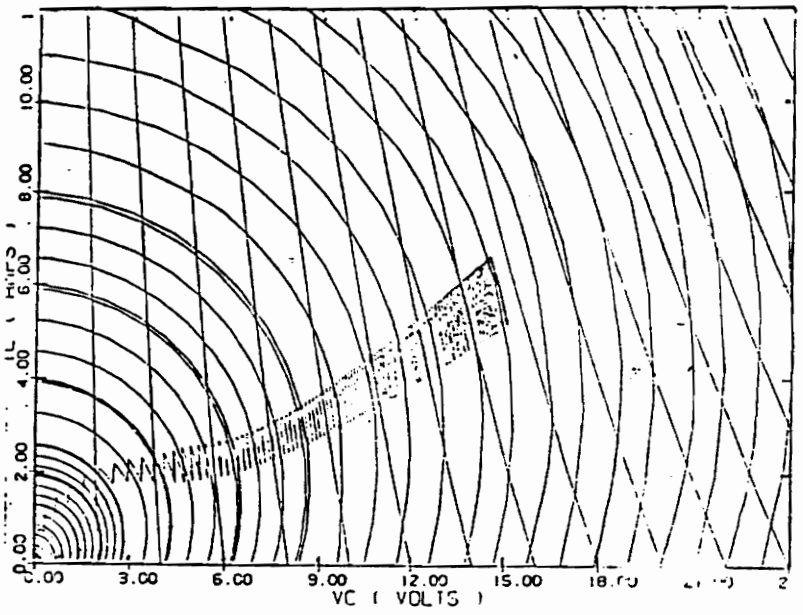

(a)

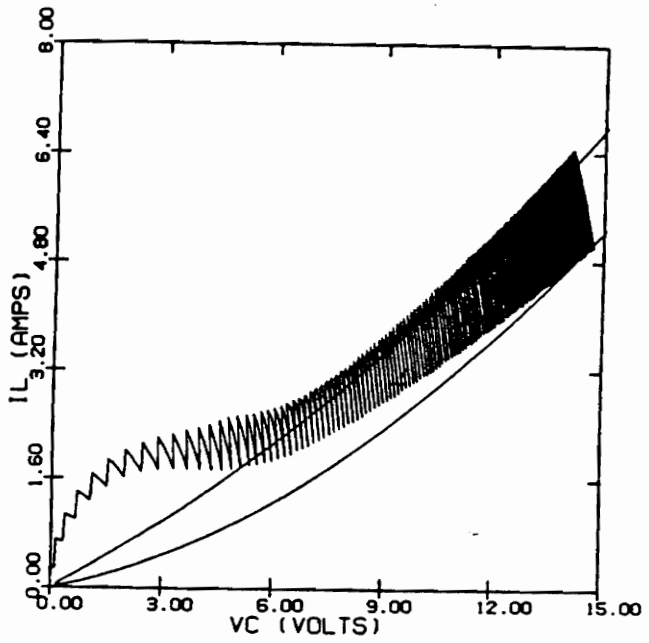

(b)

Figure 4.4 Start-up trajectory of buck/boost converter
(a) Start-up trajectory on the phase plane portrait
(b) Start-up trajectory and attraction region

Buck/boost converter Fig. 4.4 depicts the start-up trajectory of a buck/boost converter. The transition pattern of trajectory is very similar to the boost converter originating from the equilibrium of subcircuit B as shown in Fig. 2.13. As pointed out in the Chapter II, the phase-plane portrait of boost converter and buck/boost converter have same structure in the practical operating range. As a result, transient trajectories of two converters are very similar. The Fig. 4.4 (b) illustrates the qualitative behaviour of start-up trajectory in conjunction with the region bounded by envelopes.

The qualitative behaviour of start-up trajectories of converters is explained using the concept introduced in the previous chapter in this section.

4.3 Step Load Change Trajectory

One of the most important transient responses of converter is that of step-load change. Since the load of a converter is not a constant, the transient response of a converter with respect to load variation has been a great concern for the converter designer. In this section, the step-load transient response of converter will explained in phase-plane.

It is clear that a converter with a new load introduced by step change has a new phase-plane portrait. Consequently, the converter has new steady state trajectory, envelopes of trajectories and the region bounded by envelopes. The initial inductor

current and capacitor voltage are steady state values of the converter before step change.

Buck converter In the Fig. 4.5(a), the step-load change trajectories of buck converter using the current-mode control is shown. The load resistor is assumed to change from 5Ω to 1Ω abruptly. The closed path located in the lower part of these plots are the steady state trajectories of the converter before load change. Note that the transient trajectory is composed of segments of on-time and off-time trajectories of converter with $R = 1\Omega$. As time passes, the trajectory converges to the region bounded by envelopes by duty ratio tuning-mode operation.

The transient trajectories of a buck converter with step-load change from $R = 1\Omega$ to $R = 2\Omega$ are illustrated in the Fig. 4.5(b).

By comparing the trajectories in Figs. 4.5 (a) and (b), an observation can be made. While the trajectories in Fig. 4.5(a) show the capacitor voltage undershoot, the trajectories in Fig. 4.5(b) show the overshoot. The decrease of R involves the undershoot and the increase of R causes the overshoot of the capacitor voltage. The capacitor voltage undershoot and overshoot depends on the output impedance of converter. To explain this tendency in the phase-plane, let's consider Fig. 4.6. Two closed curves represent the steady state trajectories of converter with different load resistors. The upper one corresponds the steady state trajectory of converter with small R and the lower is that of converter with large R. From the phase-plane portrait of buck converter, we know that the on-time trajectories move upward in clockwise direction and the off-time trajectories travel downward also in clockwise direction within the normal operation range in the phase-plane. With the introduction of step-

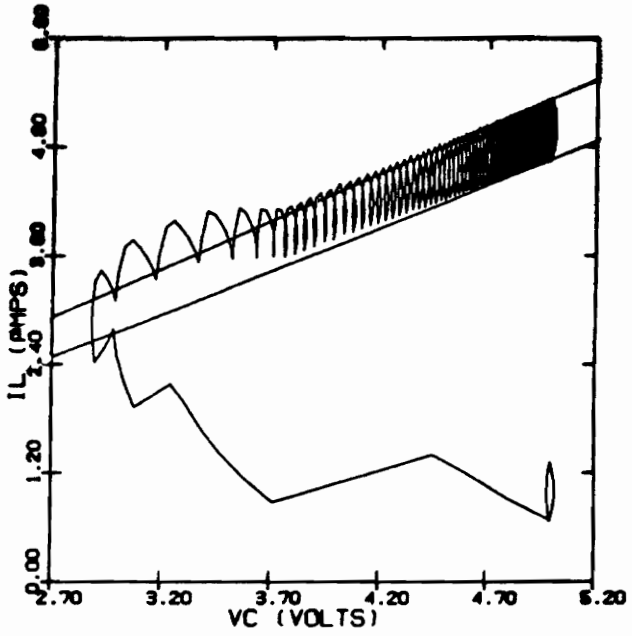

(a)

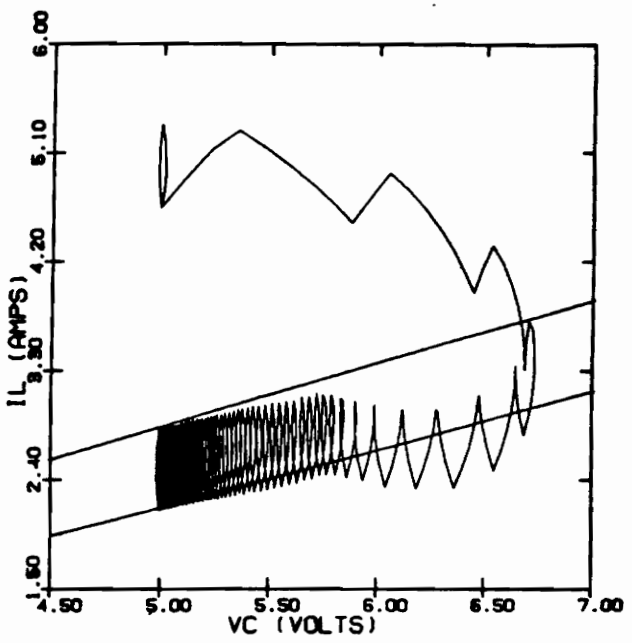

(b)

Figure 4.5 Step load change trajectories of buck converter
(a) (R : 5Ω - 1Ω)
(b) (R : 1Ω - 2Ω)

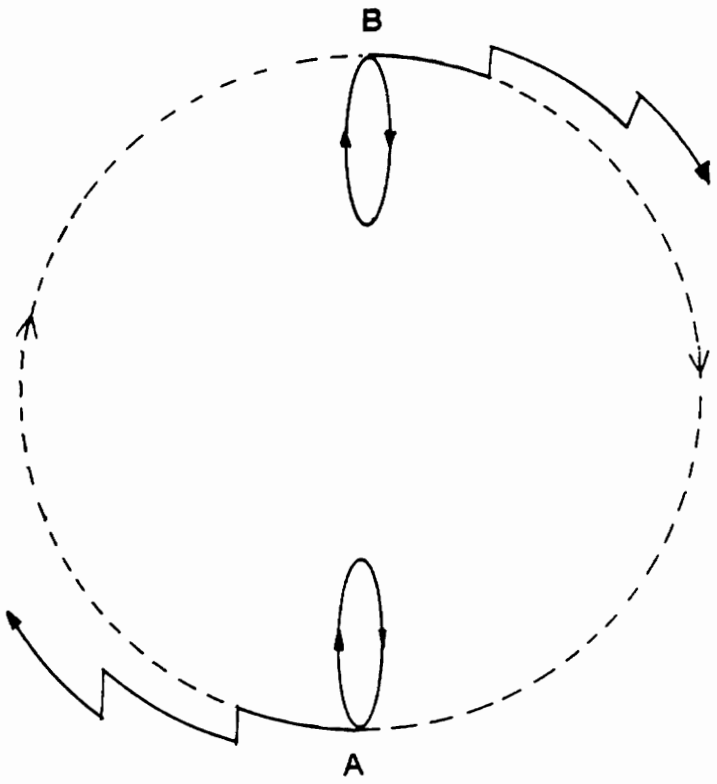

Figure 4.6 Step load change trajectories of buck converter

load change, the on-time and off-time trajectories starting out the point A and B will change accordingly. As R decreases, the on-time trajectory starting from A would rotate in clockwise direction as shown in the figure. Similarly, the off-time trajectory starting from B would rotate in clockwise direction with a larger R. It is clear that for the change of operating point from the lower trajectory to upper trajectory, there must be a net upward motion of trajectory. From Fig. 4.6, we can easily see that any effective upward motion of trajectory would result in the capacitor voltage undershoot. The ideal step-load change trajectory in the case of load stepping-up is described by the broken line assuming the trajectory would follow the on-time trajectory during the transient. In reality, the controller may generate the transistor off-command during transient due to the dynamics of feedback circuit. The trajectory drawn with solid line represents this situation. The transistor off command issued during the early stage of transient significantly increases the magnitude of undershoot and response time. One of the possible solutions of eliminating undesireable switch on-off commands during transient is to add the large-signal control law, which is effective only in a large transient, to the controller. With the large-signal control law, the transient response can be improved without changing the small-signal performance of converter.

The transition pattern of trajectory from upper trajectory to lower trajectory can be explained in the same manner. To have net downward movement, the transient trajectory should be dominated by the off-time trajectory accompanied by the capacitor voltage overshoot. The ideal transient trajectory is depicted with a broken line. Note that there is unavoidable voltage overshoot even in the ideal transient trajectory The transistor on command issued during the early stage of transition would increase the voltage overshoot and response time as illustrated with a solid line.

With the aid of Fig. 4.6, we can easily understand the step-load change trajectories of the buck converter. Furthermore, we can infer the behaviour of arbitrary transient trajectory in terms of the capacitor voltage from the above example.

Boost converter For the boost and buck/boost converters, the on-time trajectory moves upward in clockwise direction and off-time trajectory moves downward in clockwise direction. Therefore, general behaviour of transition trajectories explained before can be applied in the step-load transient of boost and buck/boost converter. Fig. 4.7 shows the step-load change transient trajectories of current-mode controlled boost converter. With the decrease of R, the trajectory yields the capacitor voltage undershoot. On the other hand, there is a overshoot with a larger R as shown. Note that the trajectory in Fig. 4.7 (c) generated with large step decrease of R shows a relatively large undershoot and slow system response.

Buck/boost converter The step-load change trajectories of buck/boost converter are illustrated in Fig. 4.8. Like the start-up case, the shape of trajectories are very similar to that of boost converter. The trajectories converges to the region bounded by envelopes showing undershoot or overshoot of the capacitor voltage as expected.

4.4 Step Input Voltage Change Trajectory

The step input voltage trajectory can be analyzed in the same way as the step-load change case. The converter after step input change has new phase-plane portrait, steady state trajectory and the region bounded by envelopes. The transient trajectory

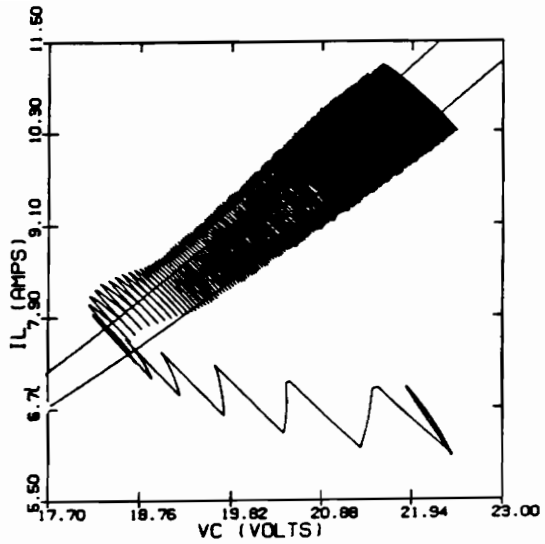

(a)

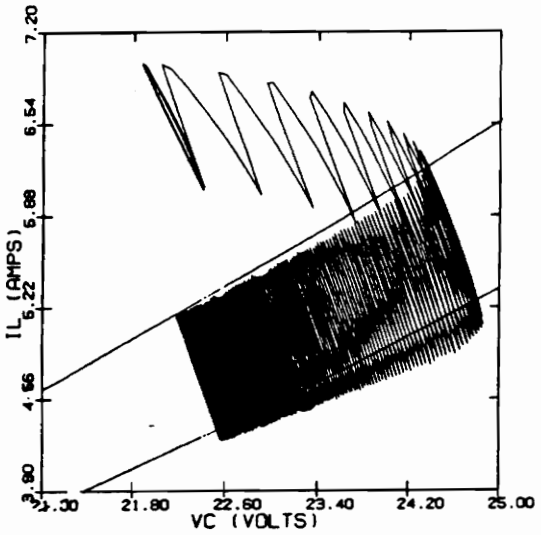

(b)

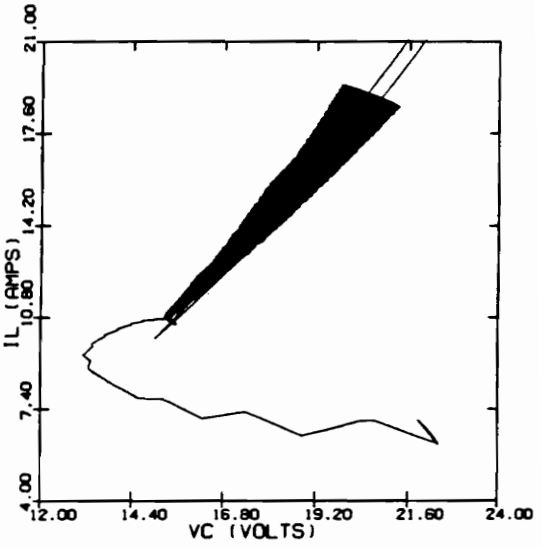

(c)

Figure 4.7 Step load change trajectories of boost converter
(a) R : 5Ω - 3Ω (b) R : 5Ω -7 Ω
(c) R : 5Ω - 1.5 Ω

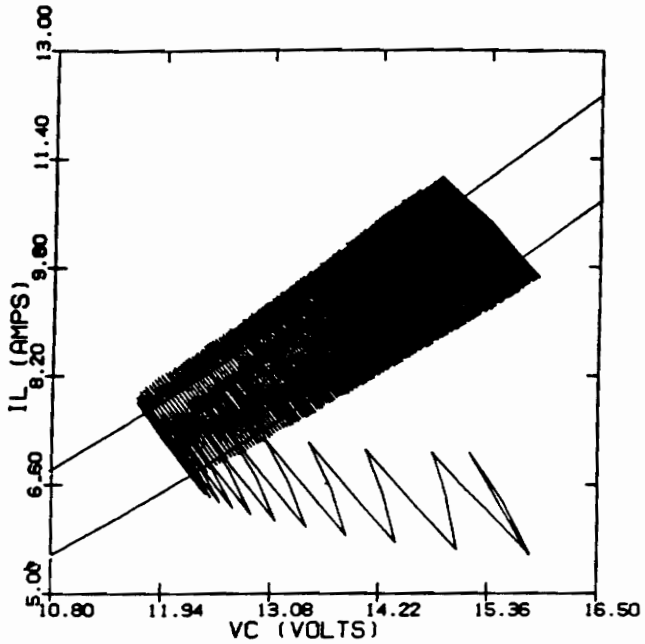

(a)

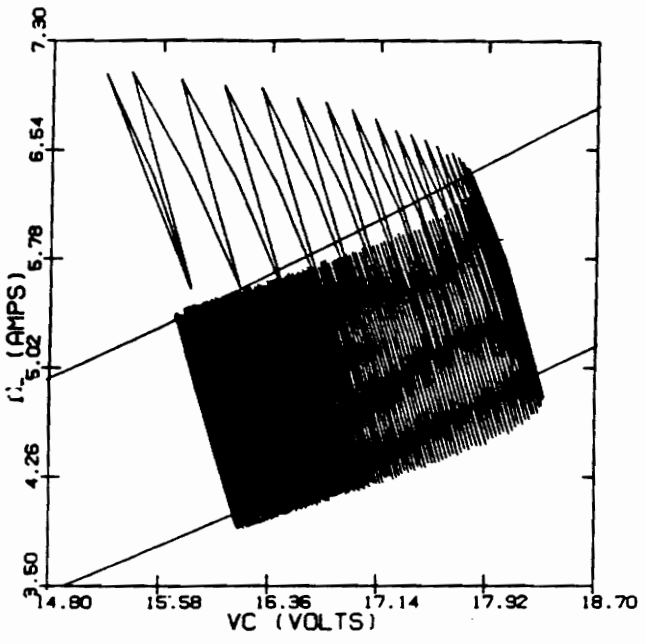

(b)

Figure 4.8 Step load change trajectory of buck/boost converter
(a) R : 5Ω - 3Ω
(b) R : 5Ω - 7Ω

can be considered as one of general transient trajectories of the converter with new input voltage.

To investigate the transition pattern of trajectories, the average inductor currents are expressed as the function of input voltage and capacitor voltage.

$$I_L = \frac{V_C}{R} \quad (Buck\ converter)$$

$$I_L = \frac{V_C^2}{V_g R} \quad (Boost\ converter)$$

$$I_L = V_C \frac{(V_g + V_C)}{V_g R} \quad (Buck/boost\ converter)$$

Whereas the average value of inductor current of buck converter is independent of input voltage, those of other converters are function of input voltage.

Buck converter Since the fundamental function of the controller is to hold the capacitor voltage as a constant regardless, of the operation condition, the location of trajectory of the buck converter remains in the same place after step input change. Fig. 4.9 illustrates this situation. Even though the trajectories show some transient response with the sudden disturbance of input voltage, they start duty ratio tuning-mode without causing large deviations of capacitor voltage due to the fact that inductor current is independent of input voltage.

Boost converter For the boost converter case, the situation is different. Since average inductor current is inversely proportional to the input voltage, the steady state trajectory will move down with the increase of input voltage. Similarly, the steady

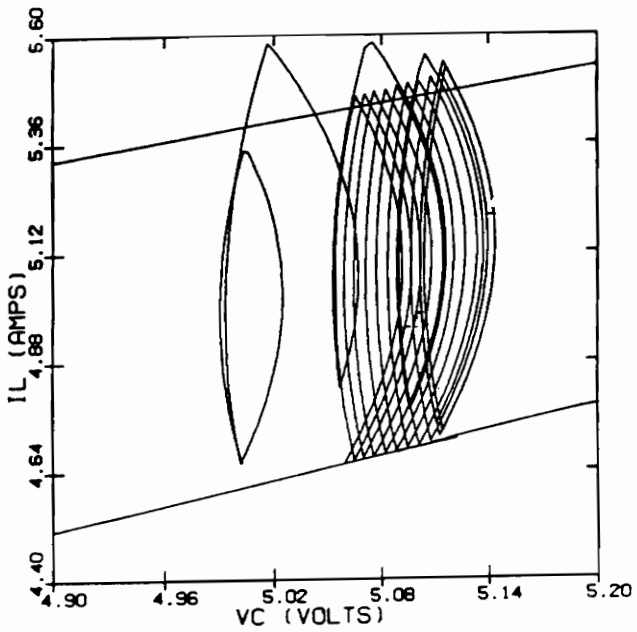

Figure 4.9 Step input change trajectories of buck converter

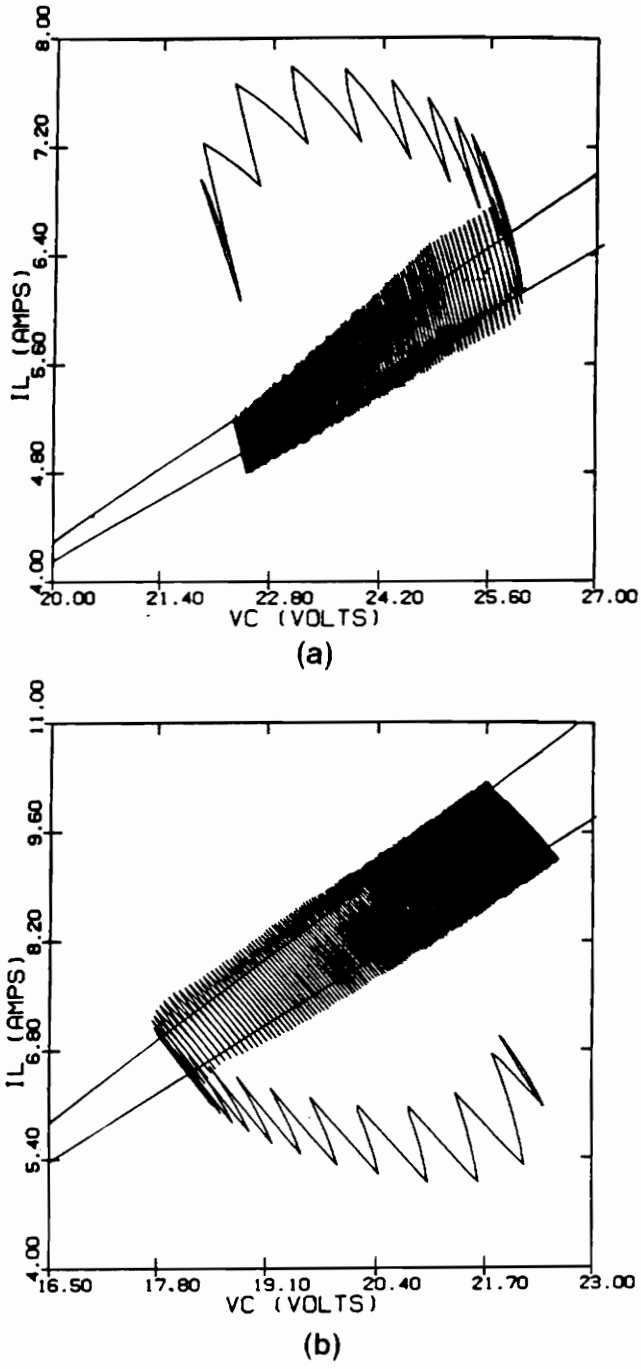

Figure 4.10 Step input change trajectories of boost converter
(a) Vg : 15V - 20V
(b) Vg : 15V - 10V

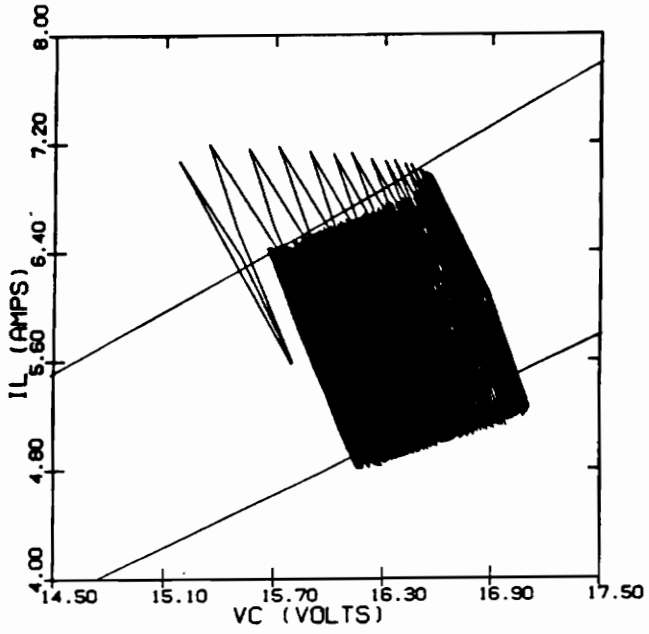

(a)

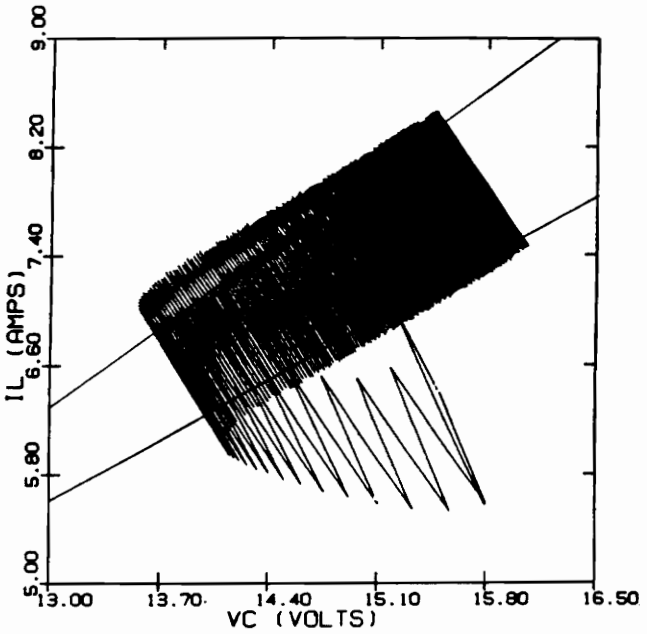

(b)

Figure 4.11 Step input change trajectories of buck/boost converter
(a) Vg : 15V - 20V
(b) Vg : 15V - 10V

state trajectory will move up with the decrease of input voltage. Therefore, the step input change trajectories behave like the step load change trajectories discussed in the previous section. As illustrated in Fig. 4.10, the capacitor voltage undergoes overshoot with large input voltage and goes through undershoot with small input voltage.

Buck/boost converter The step input change trajectories of buck/boost converter are illustrated in Fig. 4.11. Due to the dependency of the inductor current on the input voltage, the trajectories show the undershoot and overshoot of capacitor voltage respectively.

4.5 Conclusion

The large-signal transient trajectories of practical interest are investigated in the phase-plane.

The start-up trajectories are analyzed by using duty ratio tuning-mode and envelopes of trajectories. From the study of step-load transient trajectories, the following conclusion is made. The trajectory trying to increase the inductor current involves the capacitor voltage undershoot and the trajectory moving to the direction of decreasing the inductor current results in the overshoot. For the first case, any transistor off command issued in the early stage of transition significantly increases the undershoot and response time. Likewise, for the second case, the transistor on command results in an increase of overshoot and response time. These undesirable switch

on-off command can be eliminated by adding the large-signal control law, which is effective only in large transient, without changing any small signal performance of converter

The step input voltage change trajectories are analyzed by making use of the dependency of average inductor current on the input voltage. The buck converter's trajectory does not have a large excursion due to the independency of inductor current on the input voltage . On the other hand, since the inductor current is a function of the input voltage, the boost and buck/boost converters' trajectories showed a considerable excursion of capacitor voltage. The similar structure of phase-plane portraits of boost converter and buck/boost converters produced a common transition pattern of trajectories. In the step input change transient, the current-mode control results in faster response than the single-loop control because information of input voltage change directly appears in inductor current, hence, in the feedback controller, without going through the output filter stage.

V. EFFECT OF LARGE SIGNAL CHARACTERISTICS OF CONTROLLER

5.1 Introduction

The nonlinearities of controller, whether intentional or inherent, may affect the converter's dynamic behaviour in various way. For example, the soft start circuit governs the start-up trajectory and the duty ratio limitation affects the transient response greatly.

In this chapter, the effect of the large-signal characteristics of the controller on the transient response are investigated in detail. The behaviour of start-up trajectories under the control of soft start circuit is presented in the Section 5.2. Among the various nonlinearities of controller, the duty ratio limitation and the inductor current limitation are investigated in the Section 5.3 and 5.4, respectively.

Regarding computer simulation, the same circuit parameters as the previous chapter are assumed for the converters without any explicit comment.

5.2 Soft Start Circuit

In the most converter designs, it is desirable to introduce a certain type of delay, which is called soft start, during start-up for two reasons. The first is to avoid any excessive overshoot of inductor current and capacitor voltage. As discussed before, the start-up trajectory may show current and voltage overshoot without proper soft start scheme. The second reason, which is more important, is to guarantee the successful start-up of converter. As will be explained, we can not only assure the successful start-up but also predict the behaviour of start-up trajectory adequately with suitable soft start circuit.

The most common soft start strategy is to control the duty ratio to increase from zero to a desired operating value very gradually. In other words, the duty ratio during start-up is controlled in such way that it varies from zero to a steady state value slowly during the start-up process of converter. Fig. 5.1 shows how a soft start circuit may be implemented in a single-loop controlled converter. Initially the capacitor C is uncharged and the error amplifier output is held to ground through diode D_1 inhibiting the comparator output. As time increases, the capacitor starts to charge through resistor R with time constant, $\tau = RC$, toward V_{cc}. As capacitor C attains full charge, diode D_1 is reverse-biased, making the output of the error amplifier isolate from soft

start circuit. The slow charge of capacitor results in gradual increase of duty ratio as shown in Fig. 5.1.

The start-up trajectories of a buck converter with the soft start circuit in Fig. 5.1 with different time constant are shown in Fig. 5.2 where the upper and lower envelopes of limit cycles are also attached.

With the gradually changing duty ratio from zero to the steady state value, the trajectories are confined in the vicinity of the region bounded by envelopes without any large transition mode. Since the large time constant of soft start circuit implies the more gradual change of duty ratio, the trajectory approaches the region bounded by envelopes more closely as the time constant increases. Thus, with the suitable soft start circuit, the envelopes of steady state trajectories approximate the start-up trajectories. Note that the trajectory does not show any current or voltage overshoot. Furthermore, since the start-up trajectory governed by soft start circuit is inherently stable, the successful start-up is always guaranteed.

It is obvious that soft start imposes a considerable increase of rise time of output voltage, thus, a reasonable value of time constant must be selected to keep the rise time within practical limit.

5.3 Duty Ratio Limitation

In practical converter design, quite often, it is necessary to limit the duty ratio for various reasons such as a converter operating in push-pull mode. As explained be-

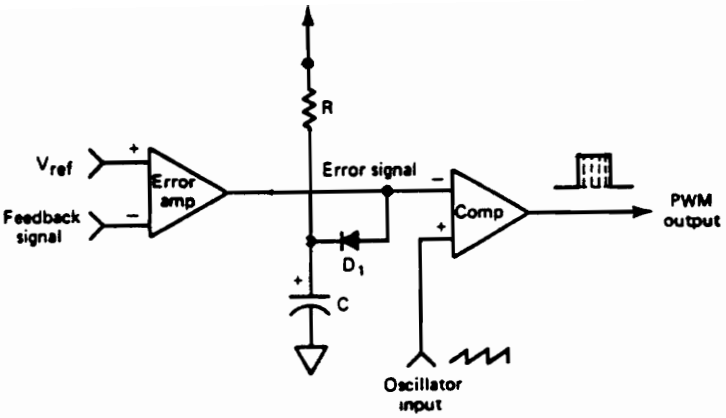

(a)

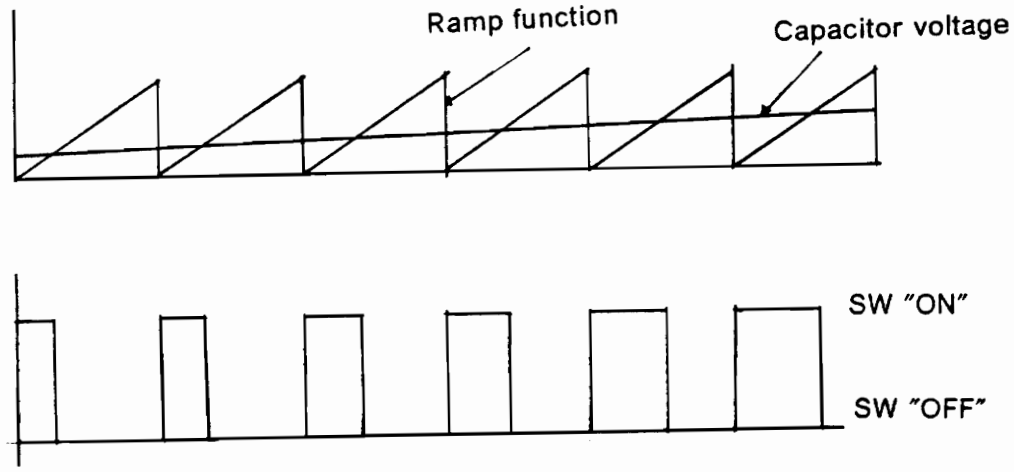

(b)

Figure 5.1 Soft start circuit
(a) Circuit schematic diagram
(b) Generation of duty ratio control signal

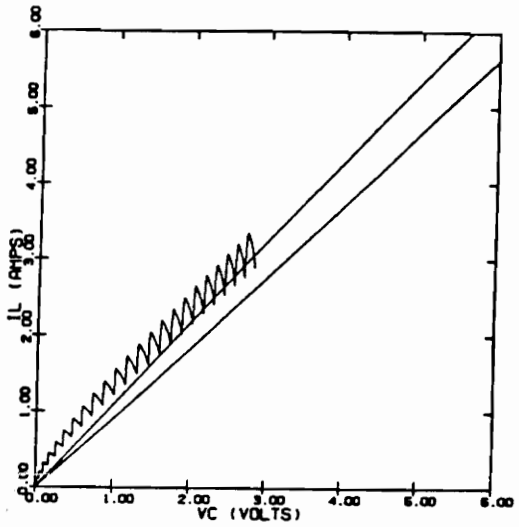

(a)

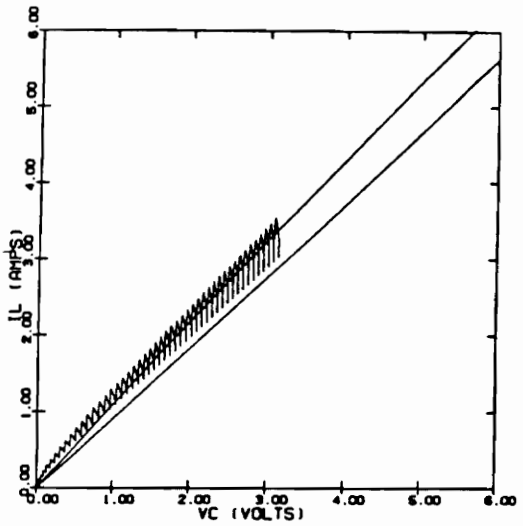

(b)

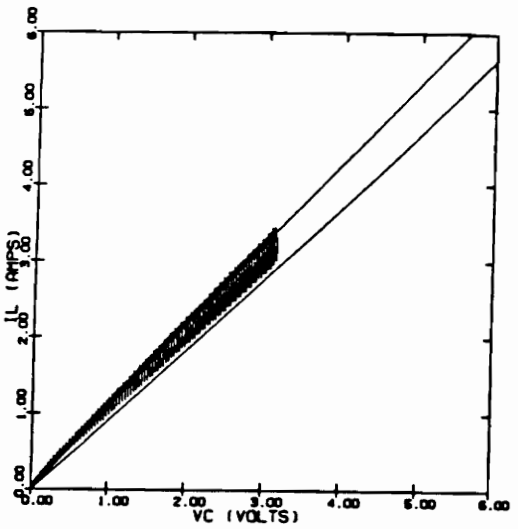

(c)

Figure 5.2 Start-up trajectories of buck converter
(a) $\tau = 0.0025$ (b) $\tau = 0.005$
(c) $\tau = 0.01$

fore, the on-time trajectory dominates the transient trajectory moving from one closed-path trajectory to another one which is located above. Likewise, the off-time trajectory dominates the transient trajectory moving down. Thus, it is obvious that the maximum value of the duty ratio, D_{max} , influences the transient trajectories moving up and the minimum value of duty ratio, D_{min}, affects the trajectory moving down. In this section, the effect of duty ratio limitation on the transient trajectory and time response is explained.

Fig. 5.3 shows the step-load change trajectories of single-loop controlled buck converter with different D_{max}. The trajectory in the Fig. 5.3 (a), assumes no limitation on the duty ratio, shows the least voltage undershoot and the smallest number of transition from one subcircuit to another during the large transition mode. As the D_{max} decreases, the trajectory shows substantial increase of voltage undershoot and the number of transition. In this case the most desirable trajectory is generated without any limitation on the duty ratio. The small value of D_{max} deteriorates the system response with the increase of the voltage undershoot. Fig. 5.4 is the time response of state of converter corresponding to the Fig. 5.3. Note that the smaller value of D_{max} increases the response time in addition to the capacitor voltage undershoot due to the frequent change of trajectory during the large transition mode.

Fig. 5.5 illustrates the influence of the minimum duty ratio , D_{min} , on the trajectory moving down. Again, the first trajectory, generated without any minimum duty ratio limitation, shows the most desireable behaviour. The voltage overshoot and response time are increasing with the larger value of D_{min} The time response of these trajectories are shown in the Fig. 5.6.

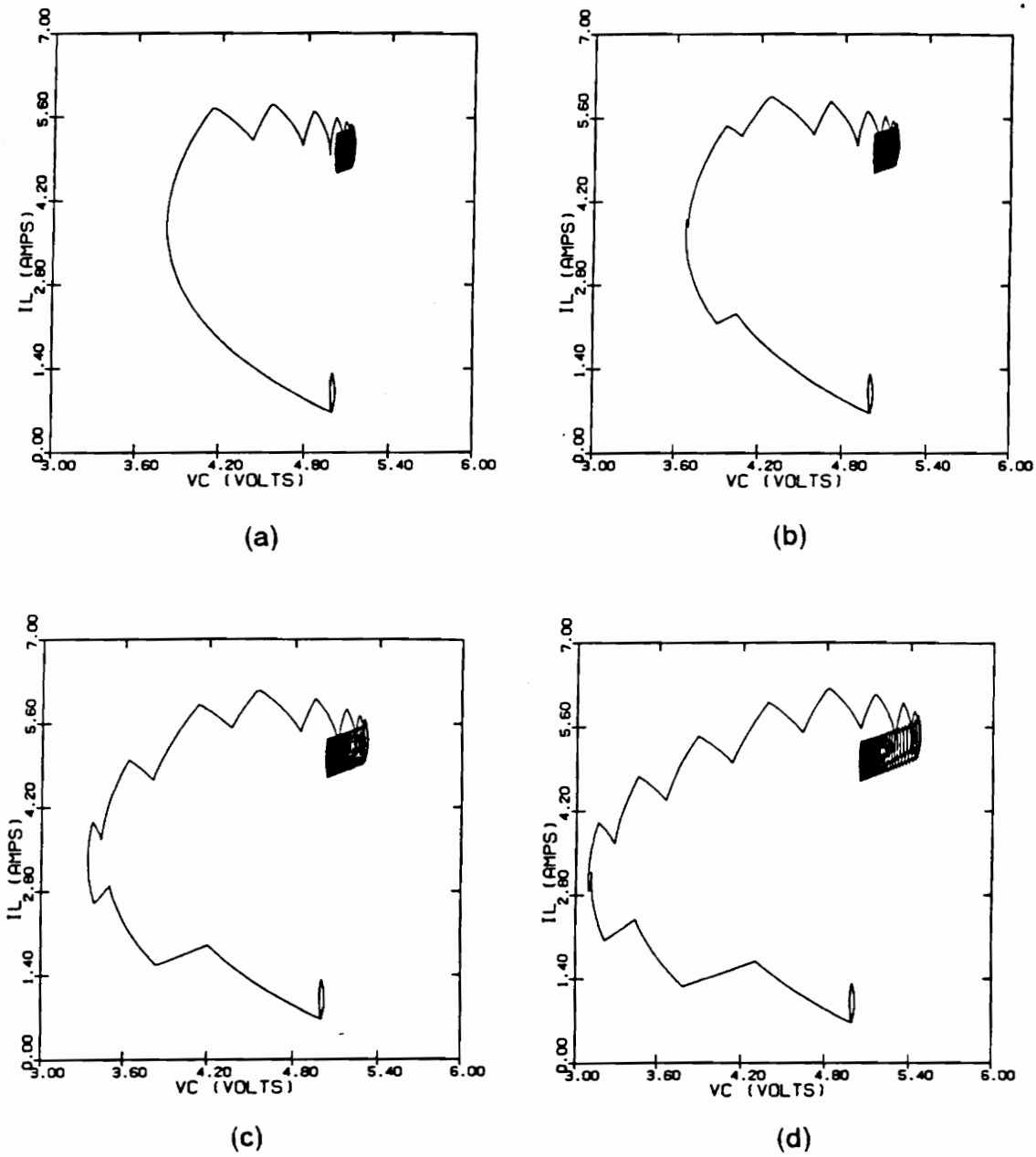

Figure 5.3 Step load change trajectories (R : 5Ω - 1Ω)
(a) $D_{max} = 1.0$ (b) $D_{max} = 0.8$
(c) $D_{max} = 0.6$ (d) $D_{max} = 0.5$

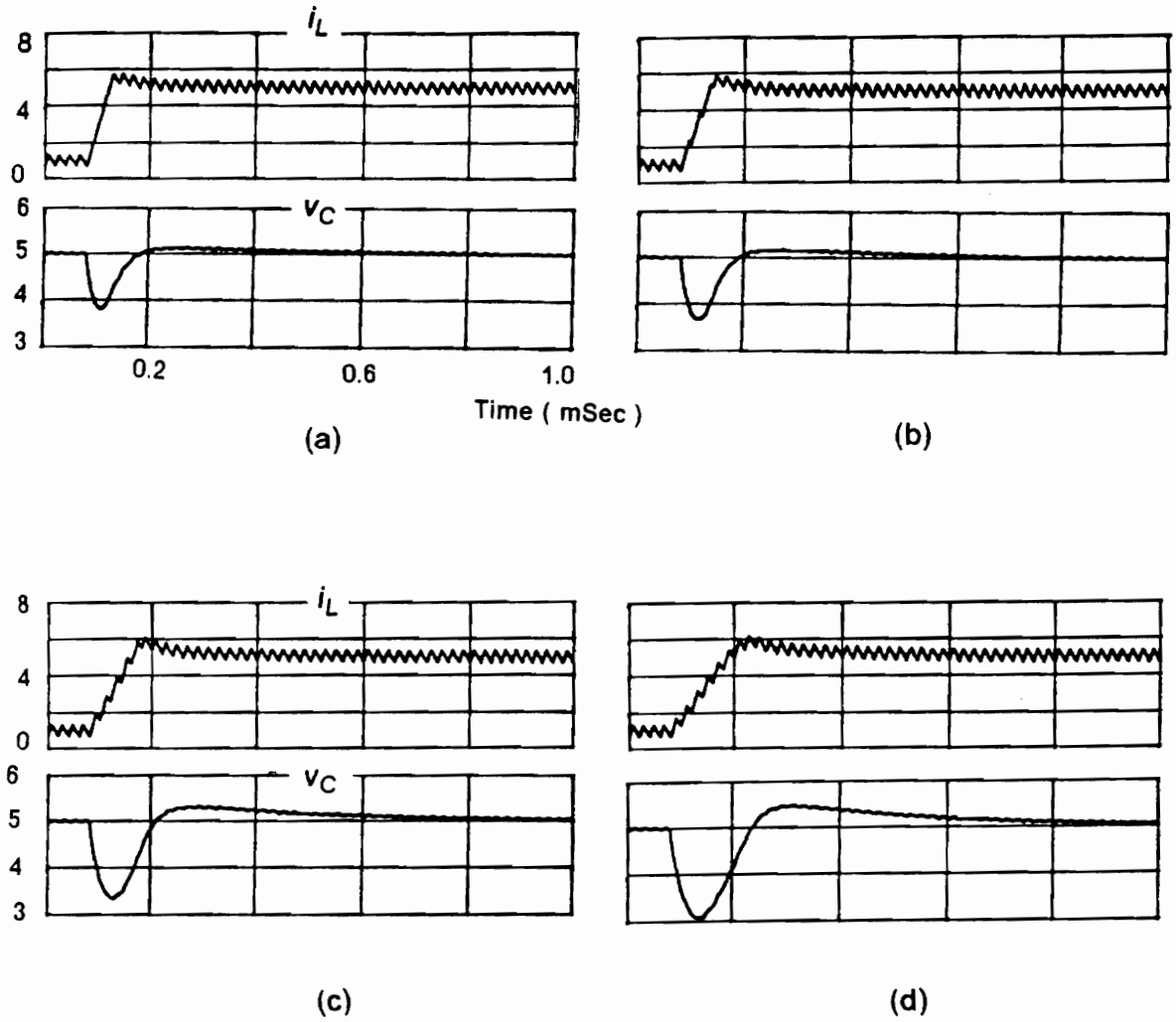

Figure 5.4 Step load change responses (R : 5Ω - 1Ω)
(a) $D_{max} = 1.0$ (b) $D_{max} = 0.8$
(c) $D_{max} = 0.6$ (d) $D_{max} = 0.5$

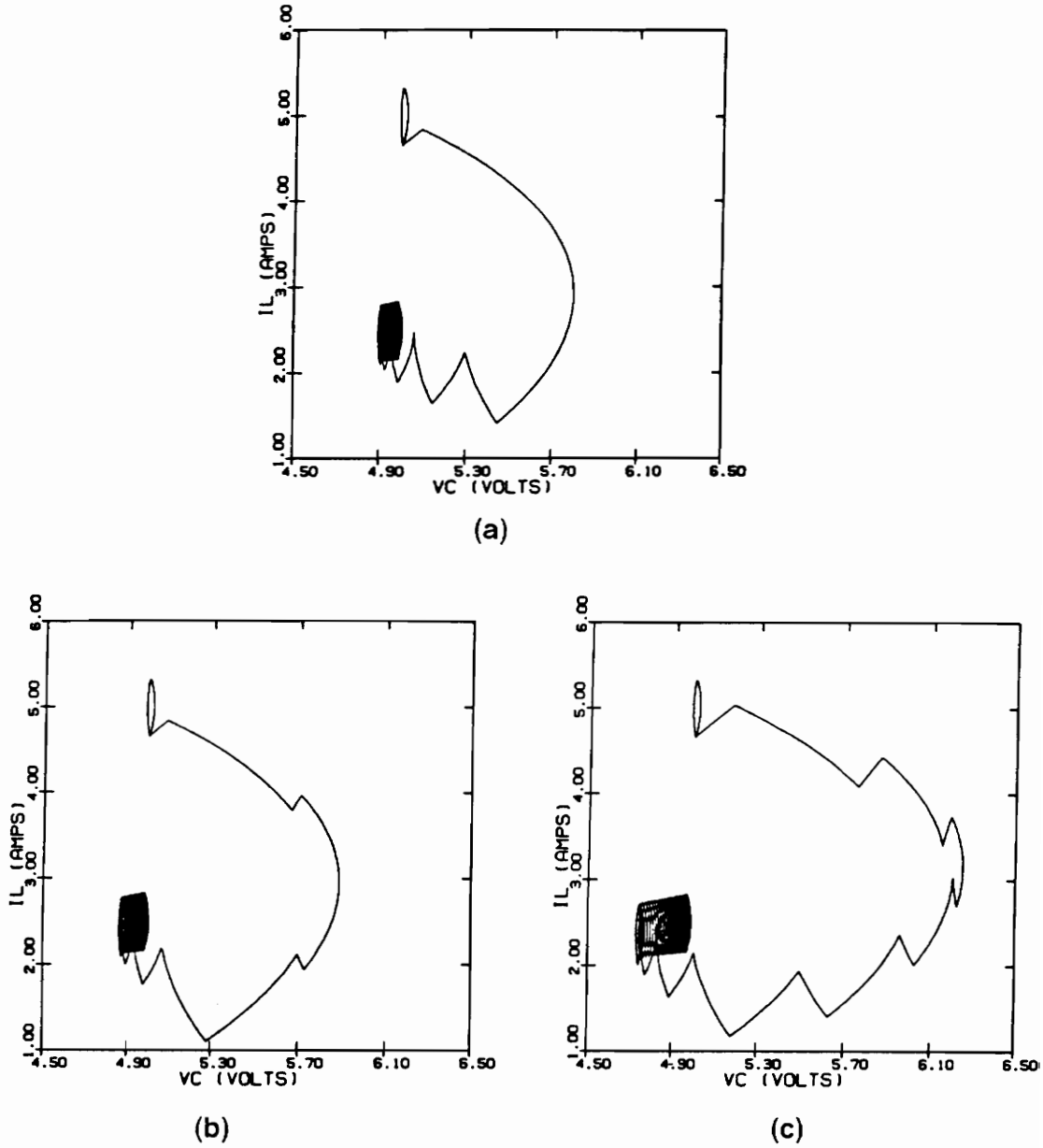

Figure 5.5 Step load change trajectories (R : 1Ω - 2Ω)
(a) $D_{min} = 0.0$ (b) $D_{min} = 0.1$
(c) $D_{min} = 0.2$

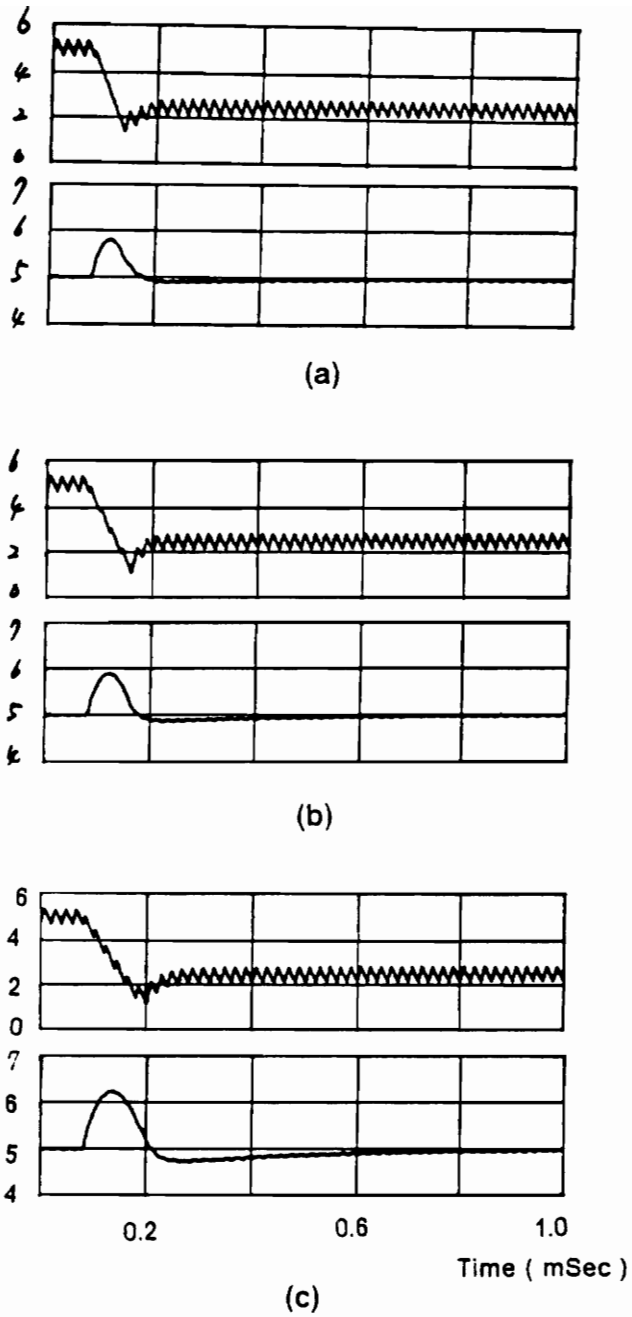

Figure 5.6 Step load change responses (R : 1Ω - 2Ω)
(a) $D_{min} = 0.0$ (b) $D_{min} = 0.1$
(c) $D_{min} = 0.2$

From the above examples, we can conclude that the limitation of duty ratio may deteriorate the large-signal response if the system is globally stable.

5.4 Maximum Current Limitation

To prevent any excessive flow of the inductor current during transient, the inductor current excursion is limit by predetermined value. Since, in three basic converters, the inductor current increases only in on-time trajectory, we can control the maximum inductor current by turn-off the switch if the current reaches to the critical value.

Due to the simplicity of the idea behind the current limitation, the effect is quite simple. Fig. 5.7 shows two step load change trajectories of a single-loop controlled buck converter. In the second plot the trajectory follows off-time trajectory as it reaches the preset maximum inductor current.

With the maximum current limitation, the response time may increase due to the large number of transitions of trajectory during the large transition mode.

5.5 Conclusion

The effect of control method and large-signal characteristics of a controller on the transient response is investigated in this chapter.

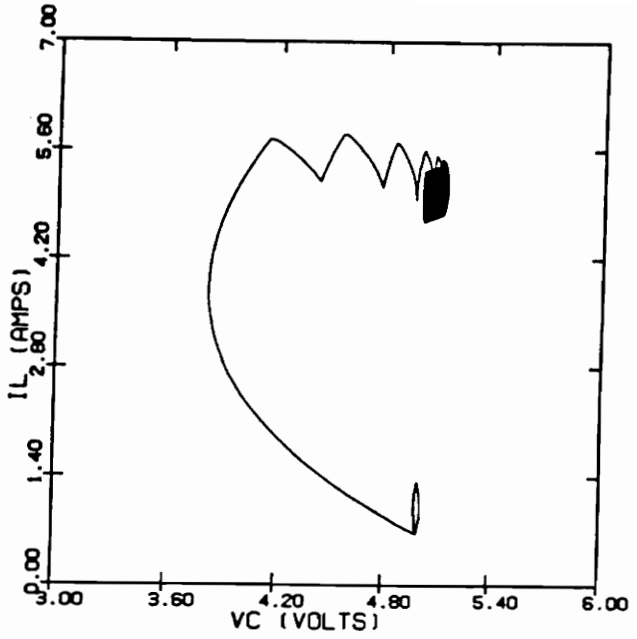

(a)

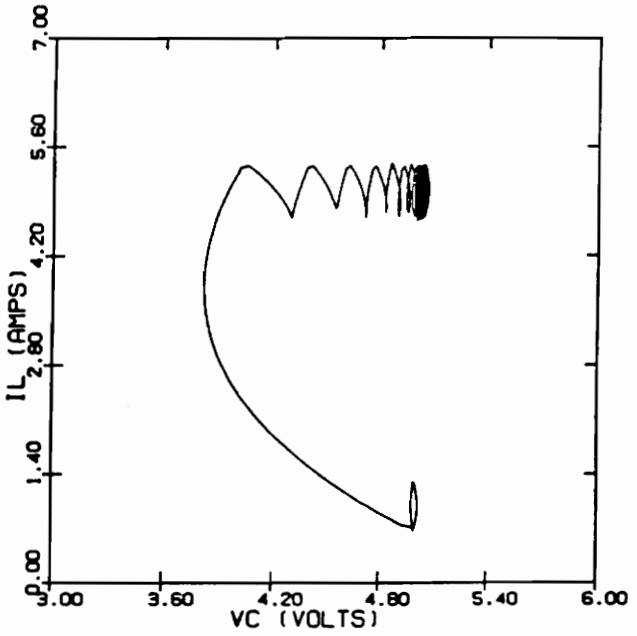

(b)

Figure 5.7 Step load change responses (R : 5Ω - 1Ω)
(a) Without current limiting
(b) $I_{max} = 5.4$

The soft start circuit produces the regular and inherently stable start-up trajectory. The limitation of duty ratio of converter imposes a considerable effect on the transient trajectories. The maximum value of duty ratio increases the response time and the capacitor voltage undershoot of trajectory which is trying to increase the inductor current. The minimum value of duty ratio increases the response time and capacitor voltage overshoot of trajectory attempting to decrease the inductor current. The peak current limiter also has similar effect as in the duty ratio limiter.

VI. CONCLUSION

In this thesis the large-signal transient response of duty ratio controlled converter is analyzed. By defining the inductor current and capacitor voltage as the state of converter, the phase-plane technique is employed.

It is shown that the behaviour of large-signal transient trajectory can be predicted in terms of circuit parameters and operating conditions. Particularly, the bounds of transient trajectories of converter with gradually changing duty ratio is identified in phase-plane. The important transient trajectories, start-up and step load/input change trajectory are analyzed. The results presented in this thesis not only provide the insight into large-signal behaviour but also can be used to generate a new large-signal control law for the optimum large-signal transient response. By adding the large-signal control law, (that is effective only in a large transient), to the feedback controller, we can control the large-signal response of converter without affecting the small signal performance. The soft start circuit is a typical example.

The main results of this thesis are summarized as follows.

The converter is viewed as a piecewise linear system changing its structure depending on the state of switches. By examining the structure of buck, boost and buck/boost converters, four subcircuits are identified. On the basis of the phase-plane analysis of those subcircuits, the composite phase-plane portraits of converters are presented. Using the phase-plane portrait of converter, the transient trajectories of converters are explained.

The concept of envelopes of steady state trajectories is developed. The envelopes define the region within which any stable trajectory would converges. The transient trajectory is divided into two parts according to variation of duty ratio. The large transition mode is characterized by the relatively large fluctuation of duty ratio. The duty ratio tuning-mode is identified by the gradual change of duty ratio. The transition pattern of arbitrary transient trajectory can be explained in terms of those two modes. A transient trajectory undergoes the large transition mode until it reach to vicinity of the envelopes of steady state trajectories. In the neighborhood of envelopes, the trajectory starts duty ratio tuning-mode showing very systematic behaviour. The unavoidable capacitor voltage overshoot or undershoot are explained according to the direction of movement of transient trajectory. The trajectory trying to increase the inductor current involves the voltage undershoot. The trajectory moving to the direction of the decreasing inductor current results in the capacitor voltage overshoot. The effect of nonlinearities of controller such as soft start circuit, duty ratio limitation is presented. The duty ratio limitation could cause a considerable increase of capacitor voltage excursion and response time.

SUGGESTIONS FOR FUTURE WORK

- The trajectory in the duty ratio tuning-mode can be related with the state space averaged small-signal model to study the validity of it in a small transient.
- The parasitic resistance of output capacitor may be included in phase-plane analysis on converters.
- The transient trajectory in the inductor current discontinuous current mode.
- The experimental verification of the transition pattern of trajectory is desired.

REFERENCES

1. D.B. Edwards and T.K. Caughey, "Global Analysis of a Buck Converter," IEEE PESC 1978 Record, June 1978.

2. R.W. Erickson, Slobodan Cuk and R.D. Middlebrook, "Large-Signal Modeling and Analysis of Switching Regulators," IEEE PESC, Record 1982, pp240-250

3. K.Harada and T. Nabeshima, "Large-Signal Transient Response of a Switching Regulator," IEEE 1981 PESC Record, pp388-394

4. W.W. Burns,III and T.G. Wilson, "State Trajectories Used to Observe and Control DC-to-DC Converters," IEEE Transaction on aerospace and Electronic Systems, Vol.AES-12, No.6, pp706-717, Nov. 1976

5. W.W Burns,III and T.G. Wilson, "Analytic Derivation and Evaluation of A State-Trajectory Control Law for DC-to-DC Converters," IEEE PESC Record 1977, pp72-85, June 1977.

6. W.W Burns, III, "A Theory of Control for A Class of Electronic Power Processing Systems: Energy-Storage DC-to-DC Converters," Ph.D. dissertation, Duke University, Durham, N.C., 1977

7. Ram. Venkataramanon, "Sliding Mode Control of Power Converters," Ph.D. dissertation, CIT, Pasadena, California, 1986

8. Boeing Computer Services Company, "Mainstream-EKS EASY5 Dynamic Analysis Systems User's Guide," April 1983

APPENDIX

A. Phase Plane Analysis of Subcircuit B

STATE EQUATION : From Figure 2.4

$$\begin{bmatrix} \dot{v}_C \\ \dot{i}_L \end{bmatrix} = \begin{bmatrix} \frac{-1}{RC} & \frac{1}{C} \\ \frac{-1}{L} & \frac{-R_l}{L} \end{bmatrix} \begin{bmatrix} v_C \\ i_L \end{bmatrix} + \begin{bmatrix} 0 \\ \frac{V_g}{L} \end{bmatrix} \qquad (A.1)$$

EQUILIBRIUM POINT :

$$v_C = \frac{R}{R + R_l} V_g$$

$$i_L = \frac{V_g}{R + R_l}$$

CHANGE OF VARIABLES : From (A.1)

$$\begin{bmatrix} \dot{\zeta}(t) \\ \dot{\eta}(t) \end{bmatrix} = \begin{bmatrix} \frac{-1}{RC} & \frac{1}{C} \\ \frac{-1}{L} & \frac{-R_l}{L} \end{bmatrix} \begin{bmatrix} \zeta(t) \\ \eta(t) \end{bmatrix} \qquad (A.2)$$

Where

$$\zeta(t) = v_C(t) - \frac{R}{R + R_l} V_g$$

$$\eta(t) = i_L - \frac{V_g}{R + R_l}$$

EIGEN VALUES : From (A.2)

$$\lambda_1 , \lambda_2 = \rho \pm i\mu$$

Where

$$\rho = \frac{-(\frac{1}{RC} + \frac{R_l}{L})}{2} \qquad < 0$$

$$\mu = \frac{\sqrt{4(\frac{1}{LC} + \frac{R_l}{RCL}) - (\frac{1}{RC} + \frac{R_l}{L})^2}}{2} \qquad > 0$$

Equation (A.2) needs to be transformed to a **canonical form** to reveal its qualitative properties directly. To do this, we need to cite two fundamental theorems.

- **Theorem 1** : A nonsingular linear transformation from $\underline{x} = \begin{bmatrix} \zeta \\ \eta \end{bmatrix}$ to $\underline{u} = \begin{bmatrix} u \\ v \end{bmatrix}$

$$\underline{u} = P\underline{x}$$

does not change the nature of equilibrium point; for example, spirals in the former plane remain spirals in the latter plane.

- **Theorem 2** : There exist a nonsingular similarity transformation Q such that the matrix $\Lambda = Q^{-1}AQ$ has the form

$$\Lambda = \begin{bmatrix} \sigma & \upsilon \\ -\upsilon & \sigma \end{bmatrix}$$

Where

$$\tau_1 , \tau_2 = \sigma \pm i\upsilon \quad \textit{are eigenvalues of matrix } A$$

By making use of theorem 1 and 2, we can transform (A.2) into following standard form.

$$\dot{\underline{u}} = \begin{bmatrix} \rho & \mu \\ -\mu & \rho \end{bmatrix} \underline{u} \qquad (A.3)$$

Where

$$\underline{u} = P\underline{x}, \qquad \underline{x} = \begin{bmatrix} \zeta \\ \eta \end{bmatrix} \quad \underline{u} = \begin{bmatrix} u \\ v \end{bmatrix}$$

From the equation (A.3),

$$\dot{u} = \rho u + \mu v$$

$$\dot{v} = -\mu u + \rho v \qquad (A.4)$$

By making use of polar coordinate for u and v , we have following relationships.

$$u(t) = r(t)\cos\theta(t)$$

$$v(t) = r(t)\sin\theta(t) \qquad (A.5)$$

Where

$$r(t) = \sqrt{u(t)^2 + v(t)^2}$$

$$\theta(t) = tan^{-1}\frac{v(t)}{u(t)}$$

From the equation (A.4) and (A.5), we have

$$\dot{u}(t) = \dot{r}(t)\cos\theta(t) - r(t)\dot{\theta}(t)\sin\theta(t) = \rho r(t)\cos\theta(t) + \mu r(t)\sin\theta(t)$$

$$\dot{v}(t) = \dot{r}(t)\sin\theta(t) + r(t)\dot{\theta}(t)\cos\theta(t) = -\mu r(t)\cos\theta(t) + \rho r(t)\sin\theta(t) \qquad (A.6)$$

By solving (A.6) for $\dot{r}(t)$ and $\dot{\theta}(t)$

$$\dot{r}(t) = \rho r(t)$$

$$\dot{\theta}(t) = -\mu \qquad (A.7)$$

From equations (A.7), we get the general solution of system.

$$r(t) = r_0 e^{\rho t}$$

$$\theta(t) = -\mu t + \theta_0 \qquad (A.8)$$

where

$$r_0 = \sqrt{u(t_0)^2 + v(t_0)^2}$$

$$\theta_0 = \tan^{-1}\frac{v(t_0)}{u(t_0)}$$

With $u(t_0) = u(t)$ *at* $t = t_0$

$v(t_0) = v(t)$ *at* $t = t_0$

Using equations (A.8), we can extract qualitative information about trajectory.

- Since $\rho < 0$, the polar radius tends to zero as t approaches to infinite.
- As t increases, $\theta(t)$ approaches to negative infinite.

Hence, the trajectory winds around the equilibrium point in clock-wise direction many times.

If we eliminates t in (A.8), the final solution of system becomes

$$r = r_0 \exp^{\frac{\rho}{\mu}(\theta - \theta_0)} \qquad (A.9)$$

and the equilibrium point is called stable **spiral point.**

B. Derivation of Envelopes of Limit Cycles

BUCK CONVERTER

Since capacitor voltage is assumed to be a constant, we have following expressions for the voltage across the inductor.

$$V_L = V_g - V_C = L \frac{\Delta i_L}{DTs} \qquad (\text{ ON TIME }) \qquad (B.1)$$

$$V_L = -V_C = L \frac{\Delta i_L}{(1 - D)\,Ts} \qquad (\text{ OFF TIME }) \qquad (B.2)$$

where

i_L : Instantaneous inductor current

V_L : Inductor voltage

V_c : Capacitor voltage

Ts : Switching period

D : Duty ratio

From (B.1), (B.2) and the flux balance requirement for inductor, we have the expression for capacitor voltage.

$$V_C = D\,V_g \tag{B.3}$$

And from (B.1), we get the expression for the peak to peak value of inductor current ripple.

$$\Delta i_L = \frac{(1-D)\,V_g D\,Ts}{L} \tag{B.4}$$

The average inducter current is equal to the load current in buck converter.

$$i_{L\,average} = \frac{DV_g}{R} \tag{B.5}$$

By making use of (B.4) and (B.5), we have the expressions for the maximum and minimum value of inductor current for a given duty ratio.

$$i_{L\,max} = \frac{\Delta i_L}{2} + i_{L\,average} = DV_g(1-D)\frac{Ts}{2L} + \frac{DV_g}{R} \tag{B.6}$$

$$i_{L\,min} = \frac{-\Delta i_L}{2} + i_{L\,average} = -DV_g(1-D)\frac{Ts}{2L} + \frac{DV_g}{R} \tag{B.7}$$

If we eliminate D in (B.3), (B.6) and (B.7), the final expression for upper and lower envelope are obtained as follows:

$$I_{upper} = \frac{V_C}{2L}\left(1 - \frac{V_C}{V_g}\right) Ts + \frac{V_C}{R} \qquad (B.8)$$

$$I_{lower} = -\frac{V_C}{2L}\left(1 - \frac{V_C}{V_g}\right) Ts + \frac{V_C}{R} \qquad (B.9)$$

Where $0 < V_c < V_g$

BOOST CONVERTER

With the constant capacitor voltage assumption, the inductor voltage can be expressed by:

$$V_L = V_g = L\frac{\Delta i_L}{D\,Ts} \qquad (\text{ ON TIME }) \qquad (B.10)$$

$$V_L = V_g - V_C = L\frac{\Delta i_L}{(1-D)Ts} \qquad (\text{ OFF TIME }) \qquad (B.11)$$

From (B.10), (B.11) and flux condition for inductor, the capacitor voltage is given by:

$$V_C = \frac{V_g}{(1-D)} \qquad (B.12)$$

By making use of the fact that forward voltage gain equals to the reverse current gain, average inductor current is expressed by:

$$i_{L\,average} = \frac{V_g}{(1-D)^2 R} \qquad (B.13)$$

Also, from (B.10), the peak to peak value of inductor current ripple is given by:

$$\Delta i_L = \frac{DTsV_g}{L} \qquad (B.14)$$

With (B.12),(B.13) and (B.14), we have final equations for envelopes of limit cycles given by:

$$I_{upper} = \frac{\Delta i_L}{2} + i_{L\,average} = \frac{V_g}{2L}\left(1 - \frac{V_g}{V_C}\right)Ts + \frac{V_C^2}{v_g R} \qquad (B.15)$$

$$I_{lower} = \frac{-\Delta i_L}{2} + i_{L\,average} = -\frac{V_g}{2L}\left(1 - \frac{V_g}{V_C}\right)Ts + \frac{V_C^2}{v_g R} \qquad (B.16)$$

Where

$$V_g < V_c$$

BUCK/BOOST CONVERTER

With same assumptions used buck converter case, the inductor voltage is given by:

$$V_L = V_g = L\,\frac{\Delta i_L}{DTs} \qquad (\text{ ON TIME }) \qquad (B.17)$$

$$V_L = -V_C = L\,\frac{\Delta i_L}{DTs} \qquad (\text{ OFF TIME }) \qquad (B.18)$$

From (B.17) and (B.18) and flux balance condition, we find capacitor voltage.

$$V_C = \frac{D}{1 - D}V_g \qquad (B.19)$$

In steady state, the capacitor must satisfy following the charge balance condition.

$$\int_0^{DTs} (-\frac{V_C}{R})dt + \int_{DTs}^{Ts} (I_L - \frac{V_C}{R})dt = 0 \qquad (B.20)$$

Where

I_L : *average inductor current*

$-\frac{V_C}{R}$: *on time capacitor current*

$I_L - \frac{V_C}{R}$: *off time capacitor current*

By simplifying (B.20), we get the expression for average inductor.

$$i_{L\,average} = \frac{D}{(1-D)^2}\frac{V_C}{R} \qquad (B.21)$$

From (B.17), the peak to peak value of inductor current ripple is

$$\Delta i_L = \frac{V_g}{L} DTs \qquad (B.22)$$

Using (B.19), (B.21) and (B.22), we have the final equations of envelopes as follows.

$$i_{upper} = \frac{\Delta I_L}{2} + I_{average} = \frac{V_g}{2L}\frac{V_C}{(V_g + V_C)} Ts + \frac{V_C(V_g + V_C)}{V_g R} \qquad (B.23)$$

$$i_{lower} = \frac{-\Delta I_L}{2} + I_{average} = -\frac{V_g}{2L}\frac{V_C}{(V_g + V_C)} Ts + \frac{V_C(V_g + V_C)}{V_g R} \qquad (B.24)$$

Vita

The author was born October 12, 1957 in Korea. He received his Bachelor's degree in Electronics from Hanyang University in 1980. From 1980 to 1985, he worked as a researcher for the Agency for Defense Development in Korea.

In the fall of 1985, he enrolled in Virginia Polytechnic Institute and State University to continue his study in electrical engineering. He finished the requirements for his Master's Degree of Science in March, 1988.